

SM and SUSY Higgs

at $e^+ e^- LC$

Introduction

Discovering Higgs Boson — SM —

Discovering Higgs Boson — MSSM —

Study of Higgs Properties

SM Higgs, $m_h > 2m_Z$

Study of Higgs Properties

light SM or MSSM Higgs

Conclusion

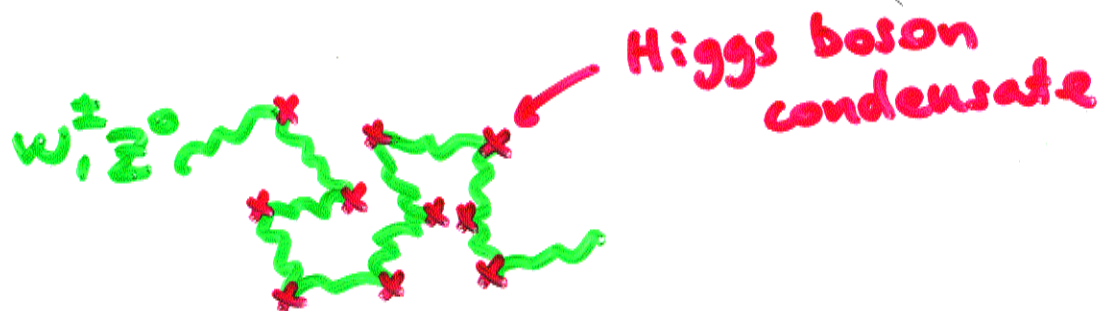
Introduction

Tevatron + LEP + SLC + NuTeV

⇒ no doubt W^\pm, Z^0 are gauge bosons

γ , graviton : gauge bosons massless

How come W^\pm, Z^0 massive?



multi-billion dollars questions:

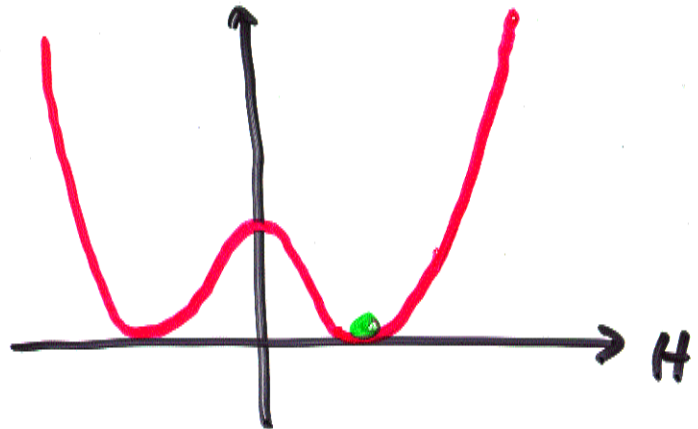
Is there really a Higgs boson?

Why does it condense?

Is it also responsible for fermion masses?

⇒ need not only to see it,
but also study it

Standard Model



$$V = \mu^2 |H|^2 + \lambda |H|^4$$
$$\mu^2 < 0$$

- only $s=0$ particle in SM
- no explanation why $\mu^2 < 0$
- radiatively unstable

UGLY!

$$\delta\mu^2 = \frac{3\Lambda^2}{16\pi^2 v^2} (2m_W^2 + m_Z^2 + m_h^2 - 4m_t^2)$$

composite Higgs

there is no $S=0$ particle

$$H \sim \bar{T}T \qquad \Rightarrow \text{chirukula}$$

supersymmetry

- many $S=0$ particles, Higgs! one of them
- radiatively stable $\delta\mu^2 \sim m_{\text{SUSY}}^2$
- dynamical explanation $\mu^2 < 0$

Λ : scale of new physics beyond SM

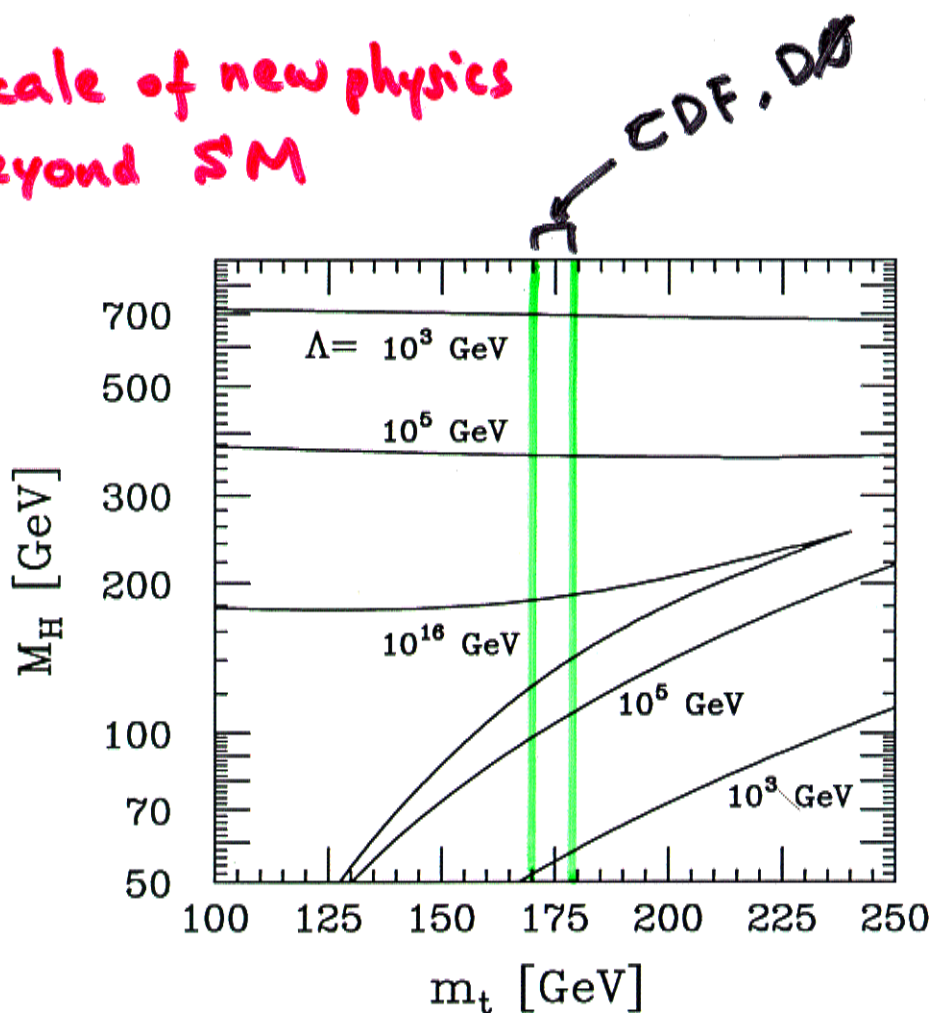


Figure 21: *Bounds on the mass of the Higgs boson in the Standard Model. Λ denotes the energy scale at which the Higgs-gauge boson system of the Standard Model would become strongly interacting (upper bound); the lower bound follows from the requirement of vacuum stability. Refs.[96, 97].*

the reconstruction of the Higgs particle.

Once the Higgs boson is found, it will be very important to explore the properties which reveal the physical nature of the particle. The zero-spin of the Higgs particle is reflected in the angular distribution of the Higgs-strahlung process which asymptotically must approach the $\sin^2 \theta$ law. Of paramount importance is the measurement of the couplings to gauge bosons and matter particles. The strength of the couplings to Z and W bosons is reflected in the size of the e^+e^- production cross sections. The strength of the couplings to fermions can be measured through the decay branching ratios and Higgs bremsstrahlung off top quarks. These measurements are important instrumentaria to establish the Higgs mechanism experimentally. Finally, the Higgs potential itself, which provides the physical basis of the Higgs phenomenon, must be reconstructed by measuring the triple and quartic Higgs self-couplings [105]. This appears possible only by exploiting multi-Higgs production in the fusion mechanism at TeV energies and maximum possible luminosity.

Minimal Supersymmetric SM (MSSM)

$$m_h \leq 130 \text{ GeV}$$

two doublets

$$\begin{array}{c} h^0, H^0, A^0, H^+, H^- \\ \hline \text{CP even} \quad \text{CP odd} \end{array}$$

parameters

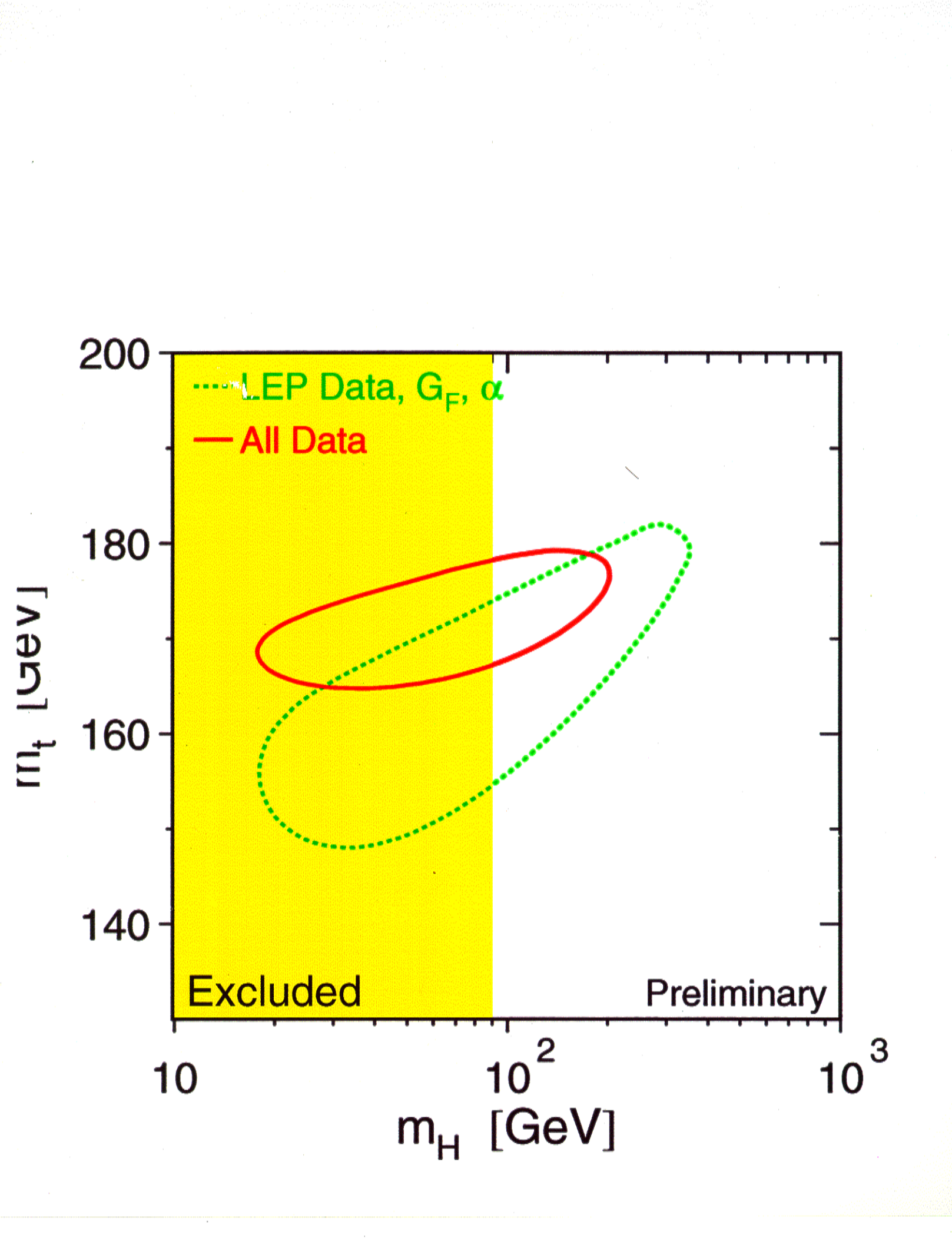
$$\tan\beta = v_u/v_d$$

$$m_{A^0}$$

$m_{A^0} \rightarrow \infty$ limit : "decoupling"

h^0 becomes SM-like

$H^0, A^0, H^+, H^- \rightarrow \infty$ almost degenerate



EW precision constraint not w/o loopholes
if new physics @ Λ

$$\Delta \mathcal{L} \sim \frac{1}{\Lambda^2} H^+ W_{\mu\nu} H B^{\mu\nu} \text{ etc}$$

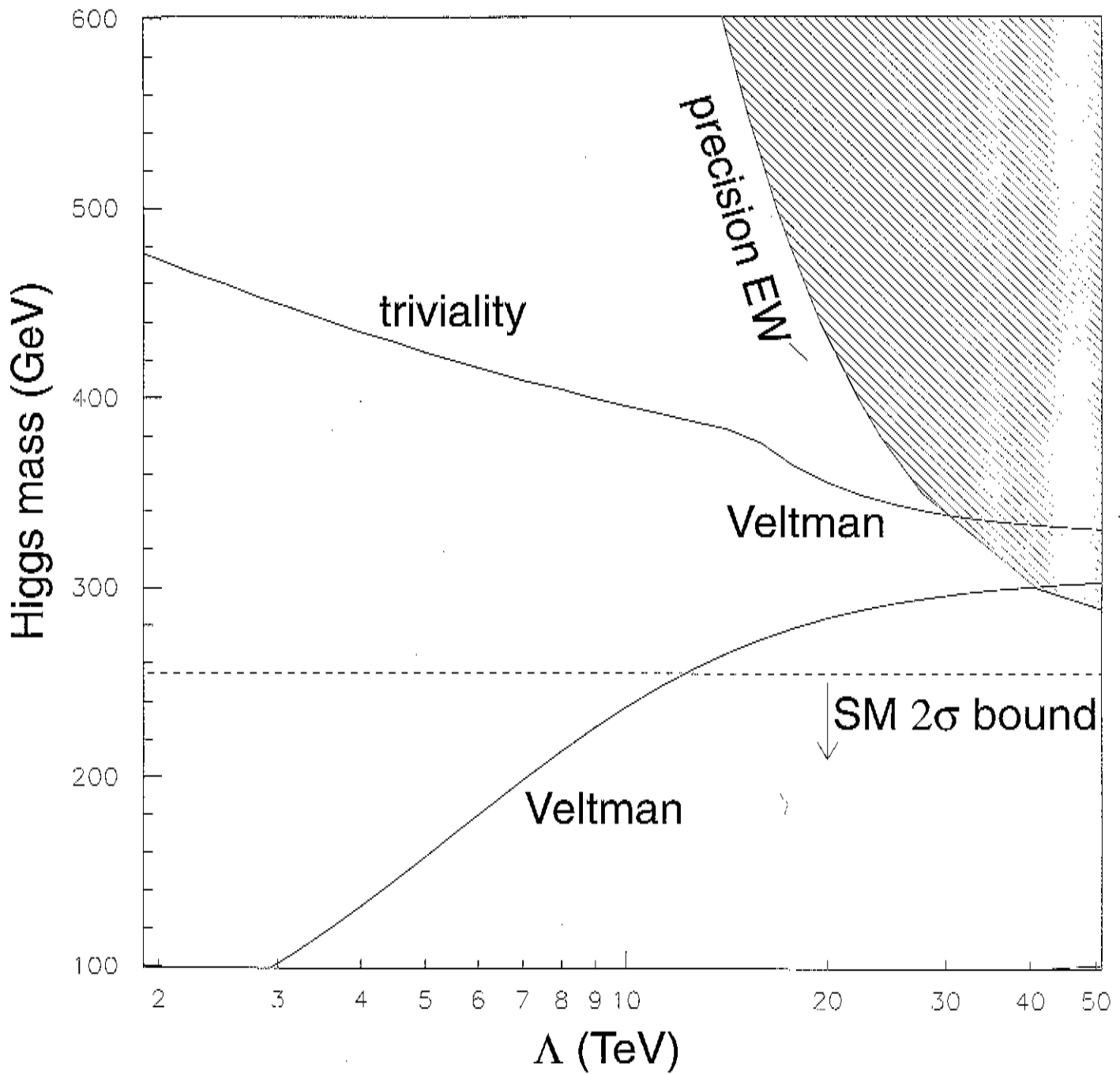
can weaken the constraint

Hall, Kolda

- requires a specific sign
- no concrete model
- don't want other operators of similar orders of magnitudes
- possible models either give the wrong sign and/or generate other unwanted operators

nonetheless, still a possibility
phenomenologically

1/10 fine-tuning allowed in Veltman condition



What can an e^+e^- LC do?

$$\sqrt{s} = 300 \text{ GeV} - 1.5 \text{ TeV}$$

\downarrow
 50 fb^{-1}

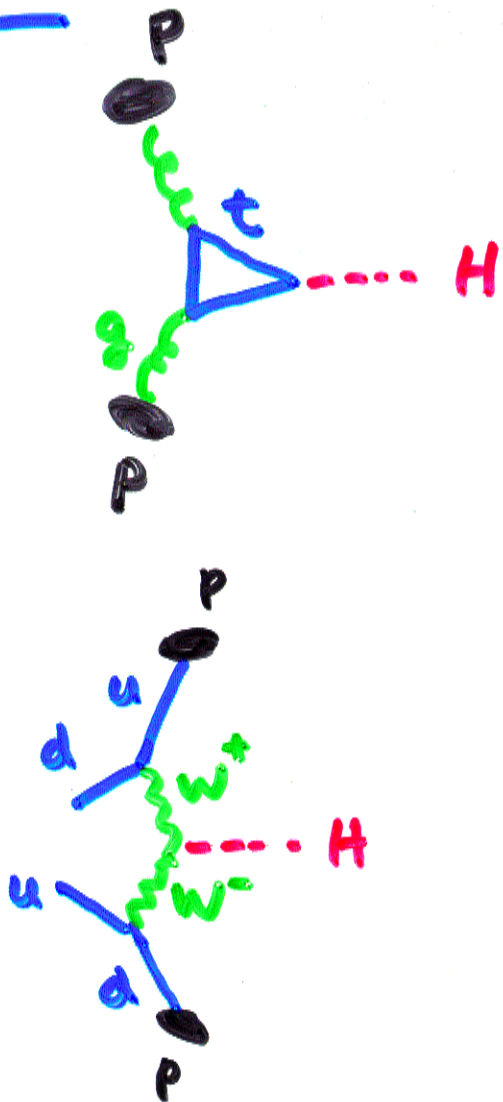
per 1 year $\approx 10^7$ sec

($\frac{1}{3}$ duty factor)

Discovering Higgs Boson

— SM —

LHC



rate very high in general

⇒ question: decay modes

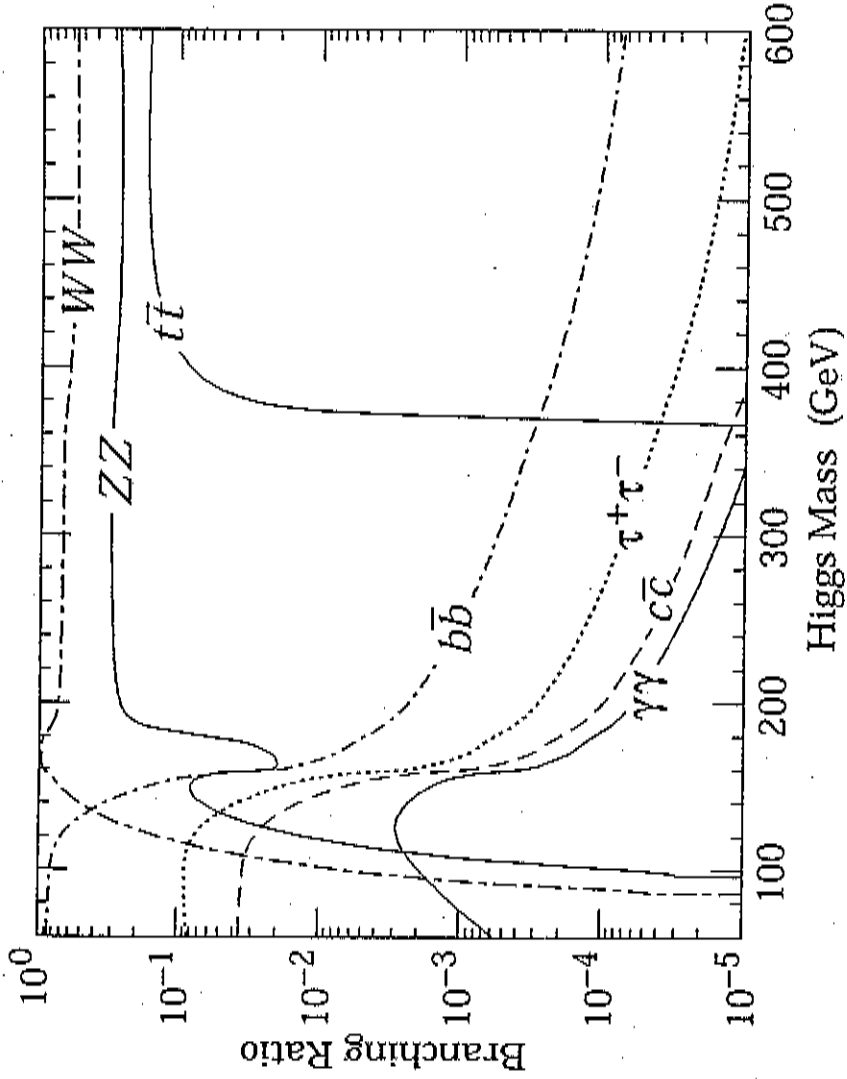


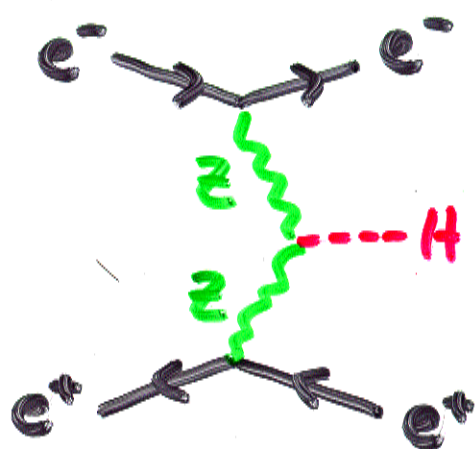
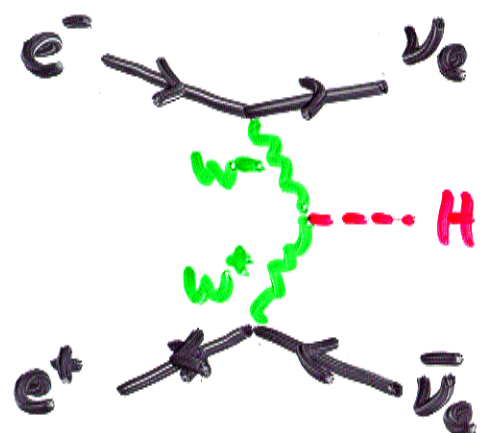
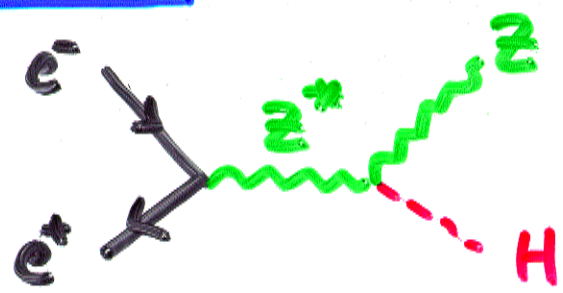
Figure 1: The branching ratio of the Higgs boson into $\gamma\gamma$, $\tau^+\tau^-$, $b\bar{b}$, $t\bar{t}$, $c\bar{c}$, ZZ , and WW as a function of the Higgs mass. For ZZ and WW , if $M_H < 2M_Z$ (or $M_H < 2M_W$), the value indicated is the rate to ZZ^* (or WW^*) where Z^* (W^*) denotes a virtual Z (W). The $c\bar{c}$ rate depends sensitively on the poorly-determined charmed quark mass.

3 LHC yrs

→ cover

μ_H > 600 GeV

$e^+ e^- LC$



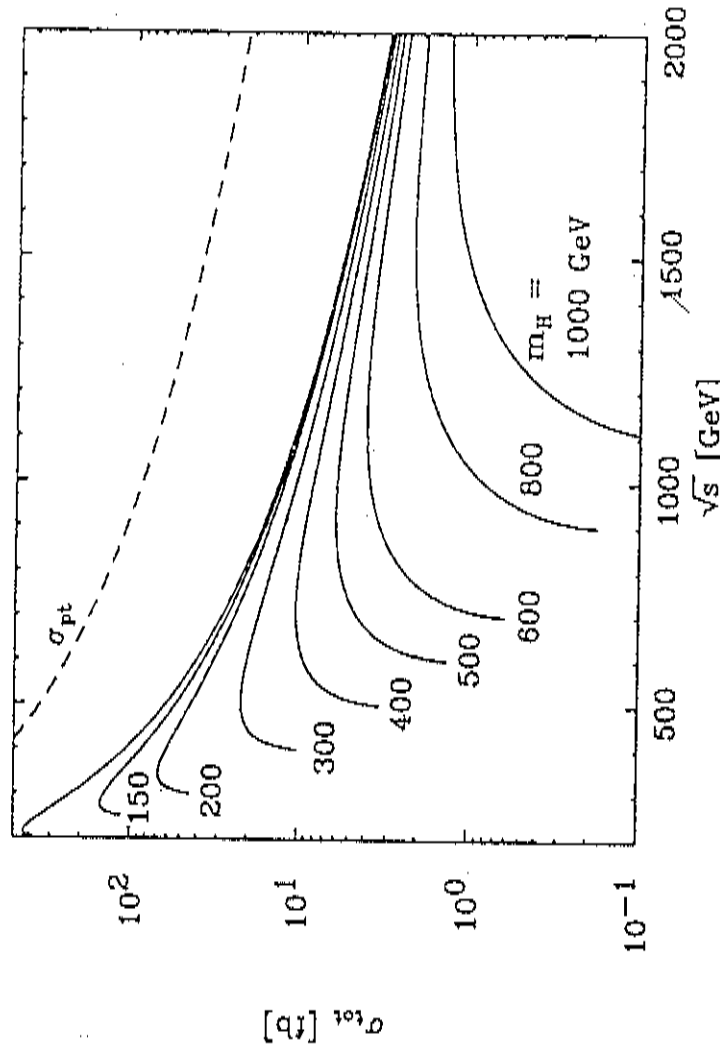


Figure 5.3: Total cross section of the process $e^+e^- \rightarrow ZH$ for various mass of the Higgs boson.

Higgs boson. However, even at this energy, the ZH production will play an important role to serve a cross-check to establish the Higgs boson.

Now we discuss the distributions of the final state particles separately.

5.2.1 $e^+e^- \rightarrow ZH$

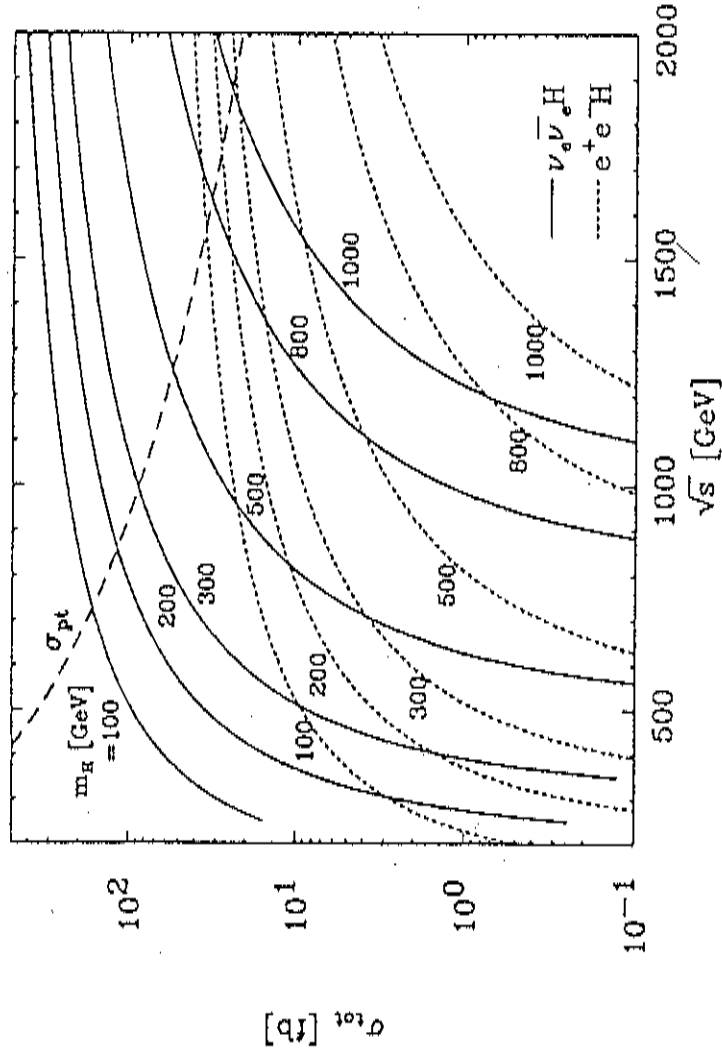


Figure 5.6: Total cross sections of the processes $e^+e^- \rightarrow \nu_e \bar{\nu}_e H$ and $e^+e^- H$ for various m_H .

important clue from the simple two-body kinematics, that the energy of the Z -boson is completely fixed to be

$$E_Z = \frac{\sqrt{s}}{2} \left(1 + \frac{m_Z^2}{s} - \frac{m_H^2}{s} \right), \quad (5.3)$$

which can appear as a peak in the E_Z distribution even with the decay of the Higgs boson.

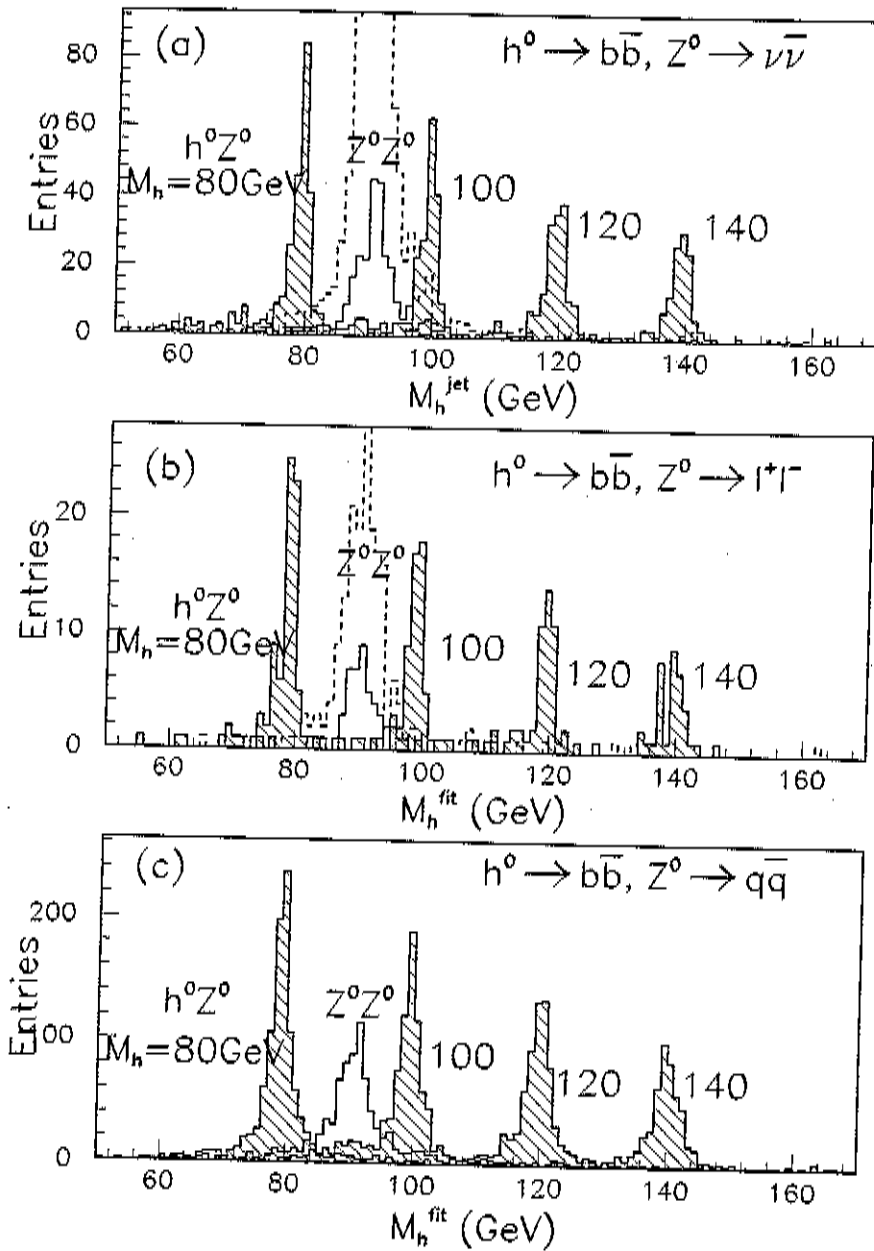
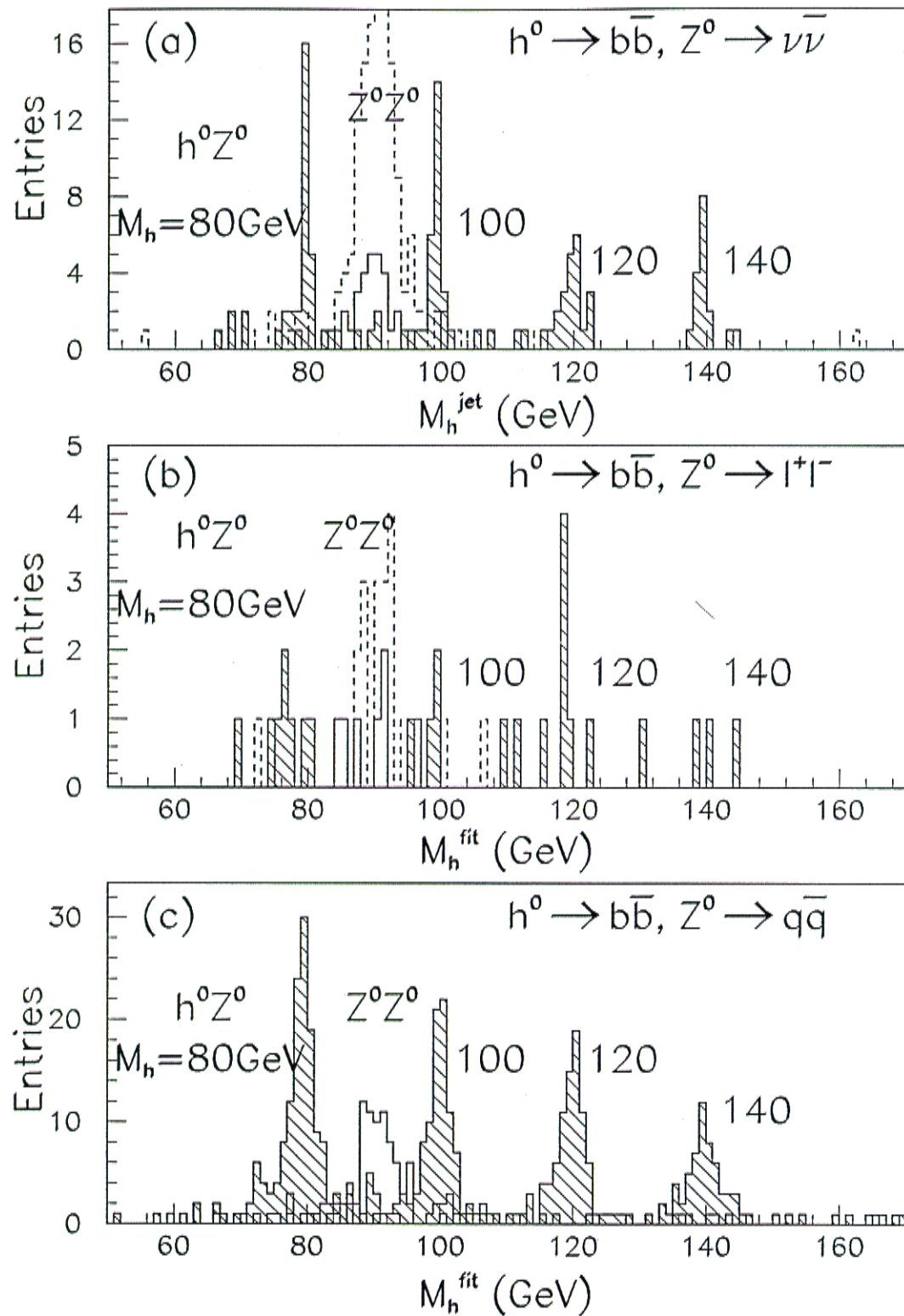
$\sqrt{s} = 300 \text{ GeV}$ 30 fb^{-1} 

Figure 12: Simulation of the detection of the Higgs boson in the process $e^+e^- \rightarrow Z^0 h^0$, from [42]. The various hatched peaks show the signal expected for a series of values of the Higgs-boson mass from 80 GeV to 140 GeV. The h^0 is assumed to decay dominantly to $b\bar{b}$; the three figures show the cases of Z^0 decay to (a) $\nu\bar{\nu}$, (b) l^+l^- , and (c) $q\bar{q}$. The dashed and solid unhatched peaks show the standard-model background without and with a b lifetime cut. The simulation assumes 30 fb^{-1} of data at 300 GeV in the center of mass.



which two thirds come from the missing energy channel, over a background of $Z\bar{q}q$ events. Only 0.8 fb^{-1} are therefore needed to observe an excess corresponding to five standard deviations above the expected background. If only the topologies giving the best mass resolution were to be kept (the leptonic channel, the four-jet topology and the $\tau^+\tau^- q\bar{q}$ final state), 1.2 fb^{-1} would suffice to reach a five standard deviation excess. The situation is even more favourable when the Higgs boson is not degenerate in mass with the Z , as shown in Fig. 7.

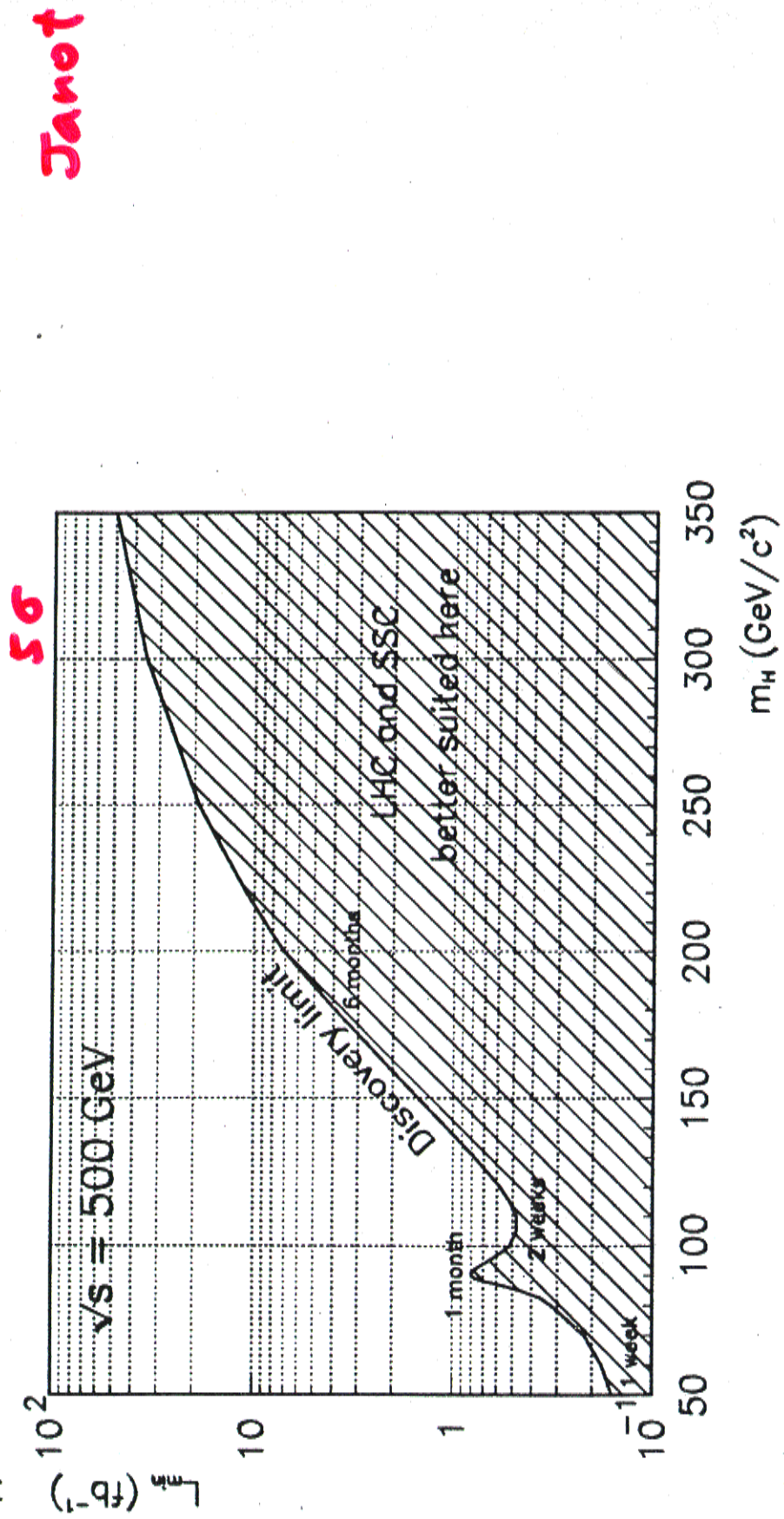


Figure 7: Minimum luminosity needed for the Higgs boson discovery.

Kurihara

H \rightarrow $W^+W^- + BG$

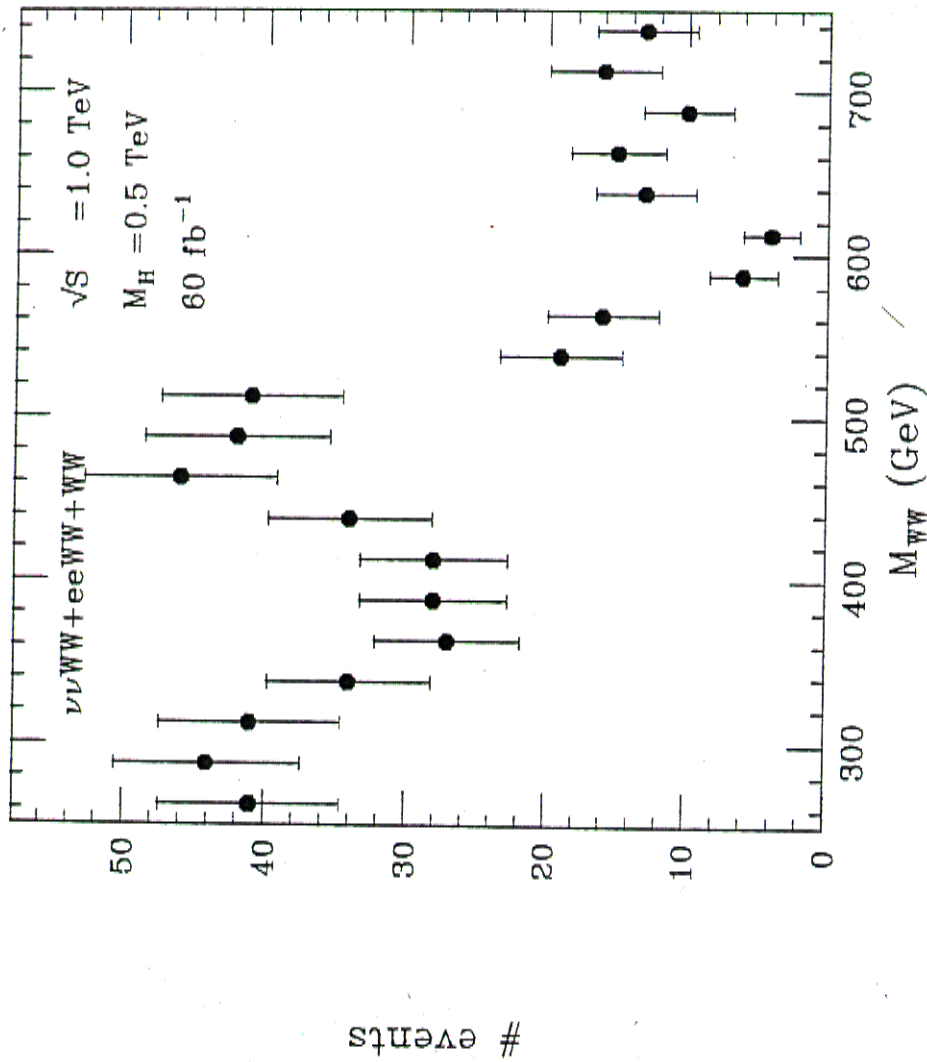


Figure 5

$L = 10 - 60 \text{ fb}^{-1}$

$\sqrt{s} = 300 \text{ GeV} - 1 \text{ TeV}$

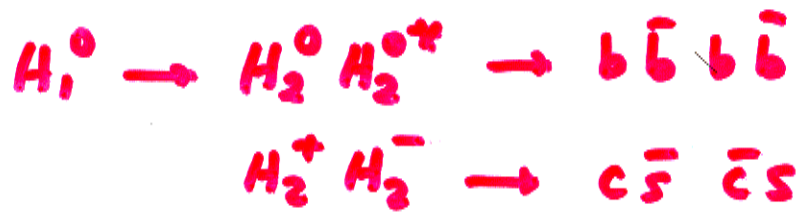
\Rightarrow SM Higgs boson
safely covered

surprise always possible

e.g. two-doublet Higgs model

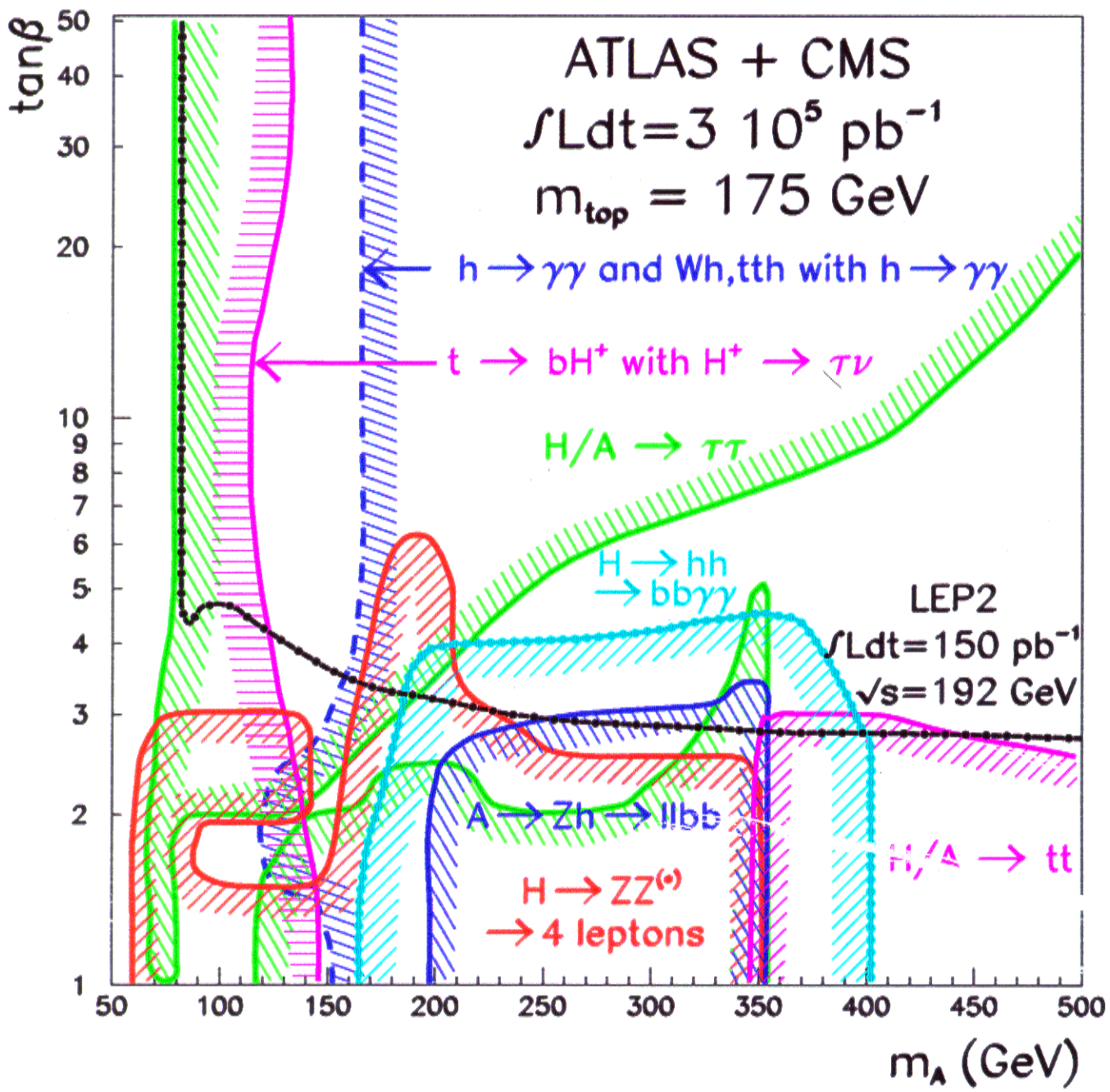
$$\langle H_1 \rangle \neq 0$$

$$\langle H_2 \rangle = 0$$

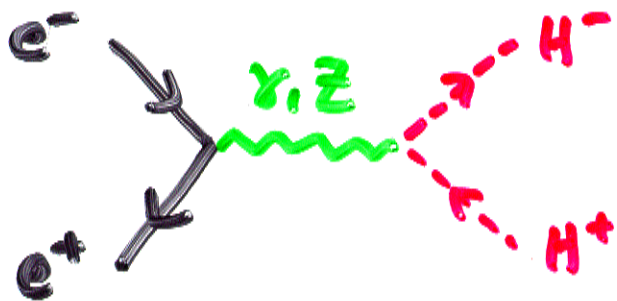
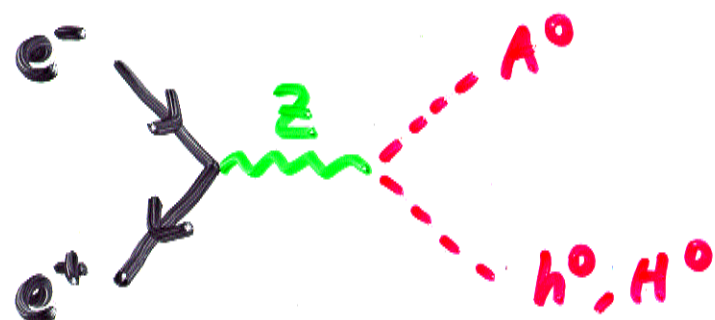
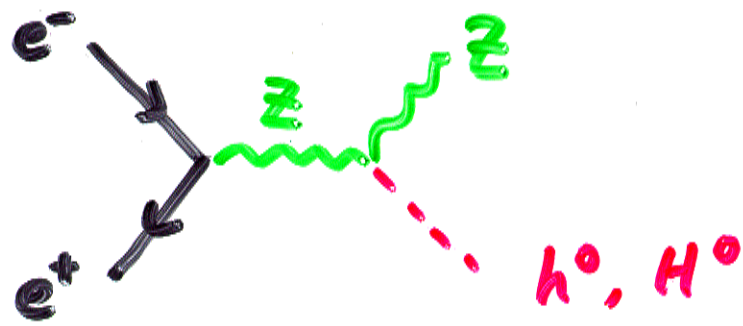


Discovering Higgs Boson

MSSM



$e^+ e^- LC$



$A^0 \rightarrow b\bar{b}, \tau^+\tau^-, \tau\bar{\tau}$

$H^0 \rightarrow b\bar{b}, \tau^+\tau^-, t\bar{t},$

w^+w^-, Z^0Z^0, h^0h^0

$H^+ \rightarrow c\bar{s}, t\bar{b}$

Janot

$Z \rightarrow jj$
 $h^0, H^0 \rightarrow b\bar{b}$

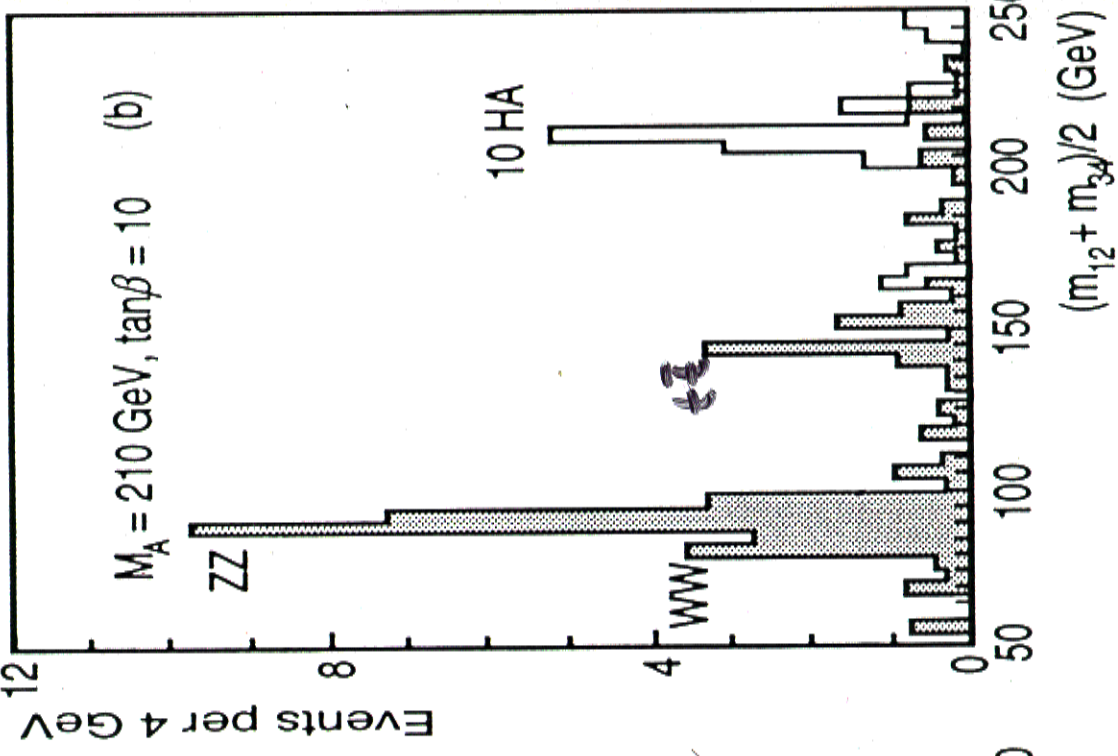
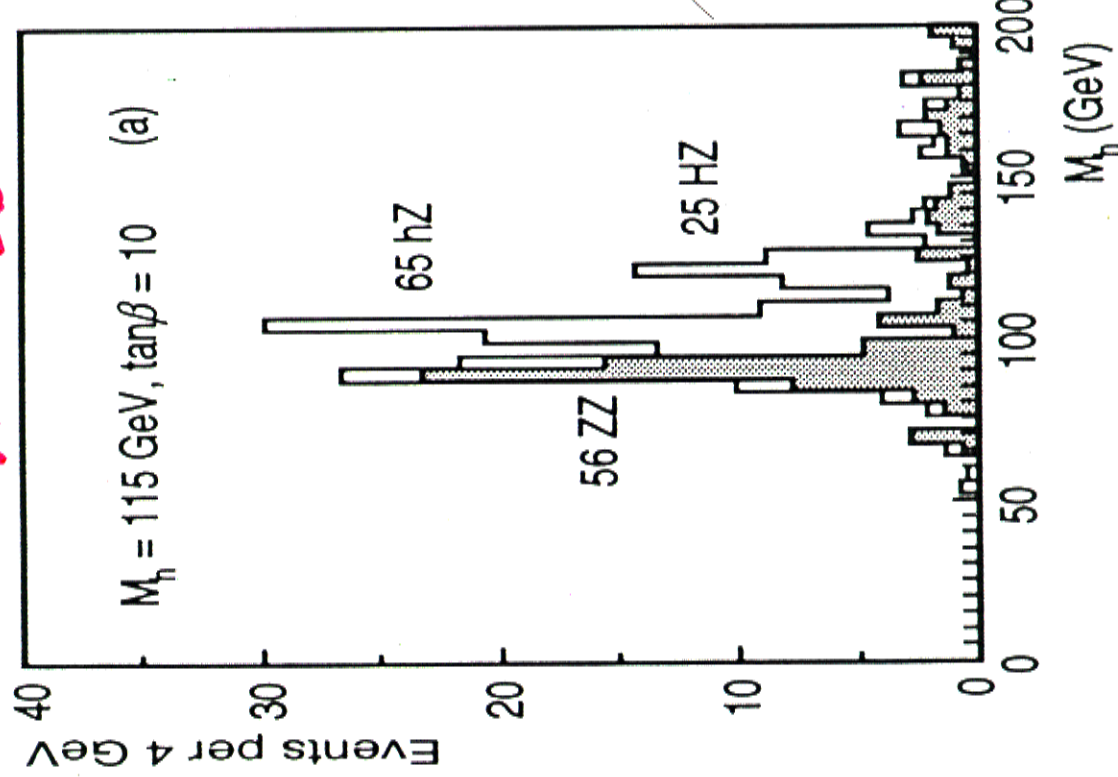


Figure 2.20: (a) Jet masses recoiling from a reconstructed Z^0 a

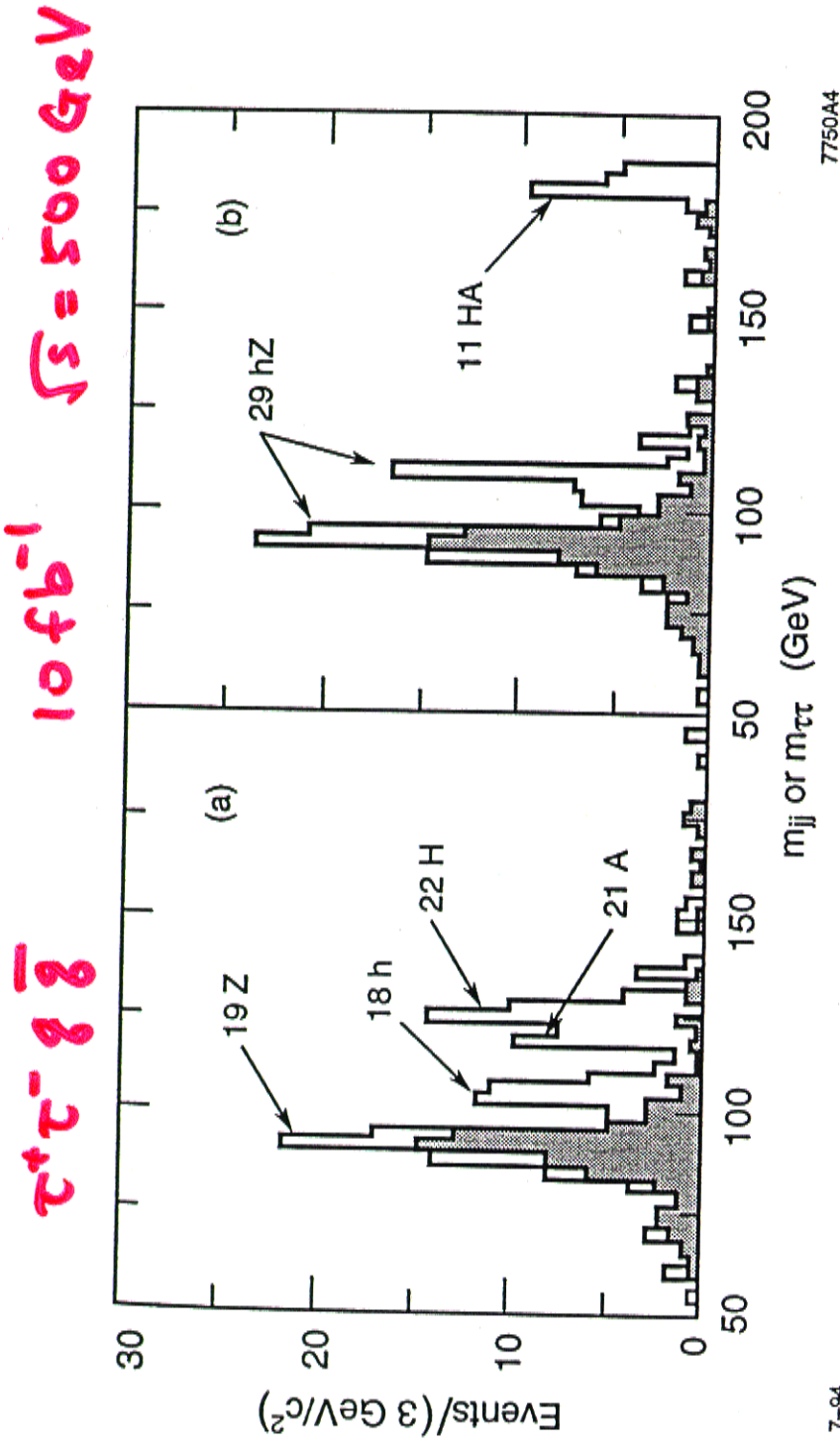
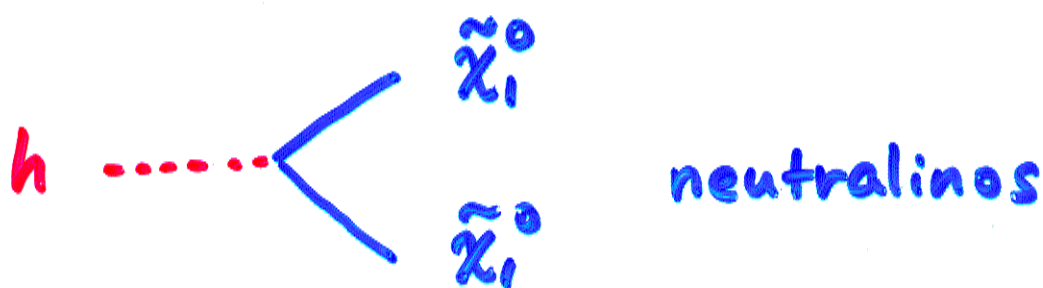


Figure 13: Reconstructed masses of Higgs and Z^0 bosons, in an analysis optimized to identify the process $e^+e^- \rightarrow b\bar{b}\tau^+\tau^-$, from [134]. The simulation assumes 10 fb^{-1} of data at 400 GeV in the center of mass. The two figures correspond to (a) $m_A = 120 \text{ GeV}$, (b) ; $m_A = 180 \text{ GeV}$. The shaded area shows the standard-model background, which comes dominantly from $e^+e^- \rightarrow Z^0Z^0$.

The cross sections for production of the MSSM Higgs bosons are presented in [136]. If the heavier scalar Higgs H^0 is relatively light, the Z receives only a fraction of its mass from the h^0 , and the cross section is correspondingly suppressed. In the region where this suppression is large, the H^0 should also be within the reach of a 500 GeV collid-

Higgs boson may decay invisibly

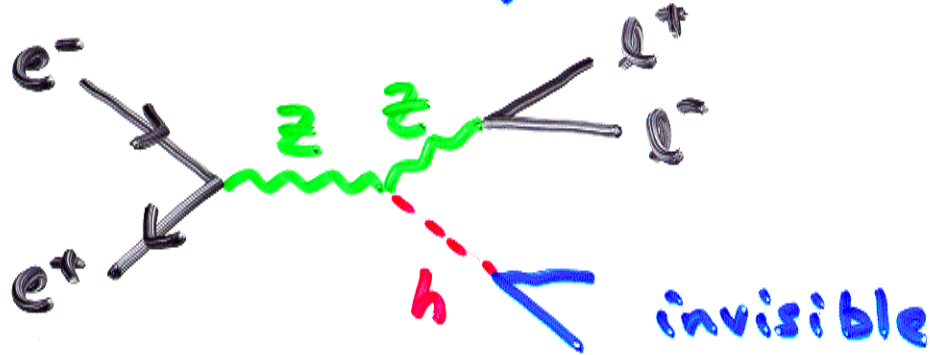


not specific to SUSY

$\nu_4 \bar{\nu}_4$

singlet Higgs

Majoron



$$E_{l^+} + E_{l^-} = E_Z = \frac{\sqrt{s}}{2} \left(1 - \frac{m_Z^2}{s} + \frac{m_h^2}{s} \right)$$

background is $e^+ e^- \rightarrow ZZ$ when one of the two Z s decays into a neutrino-pair. Altogether, 120 background events are expected with an integrated luminosity of 10 fb^{-1} , for a signal efficiency of 50%. The missing mass distribution is shown in Fig. 16 for Higgs boson masses of 110 and 140 GeV/c^2 , assuming the standard model production cross-section. To conclude, the neutral Higgs bosons of the MSSM remain “visible” even when the invisible decay is dominant.

$$10 \text{ fb}^{-1}$$

$$\sqrt{s} = 300 \text{ GeV}$$

P. Jäger

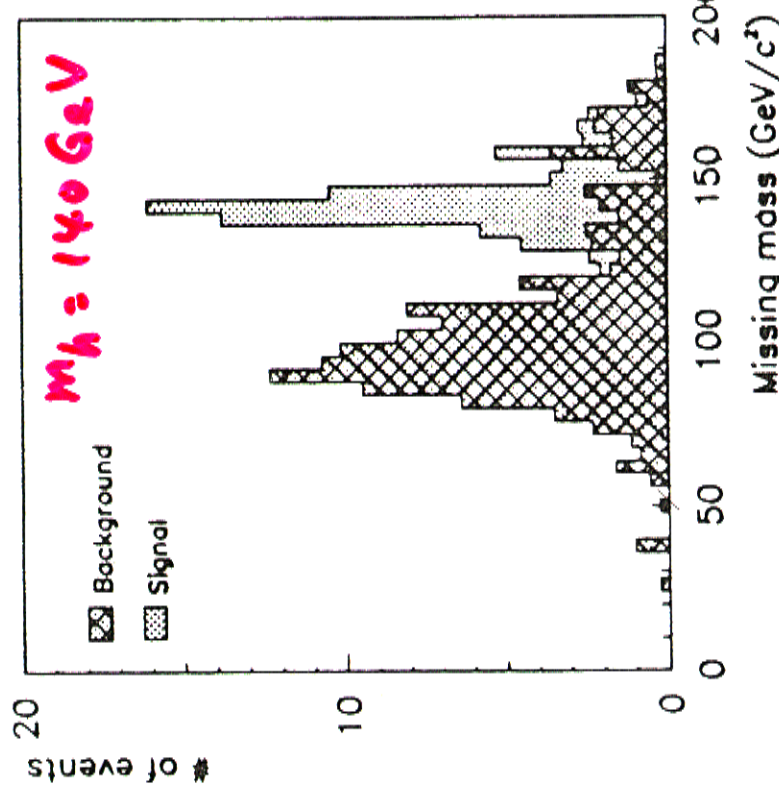
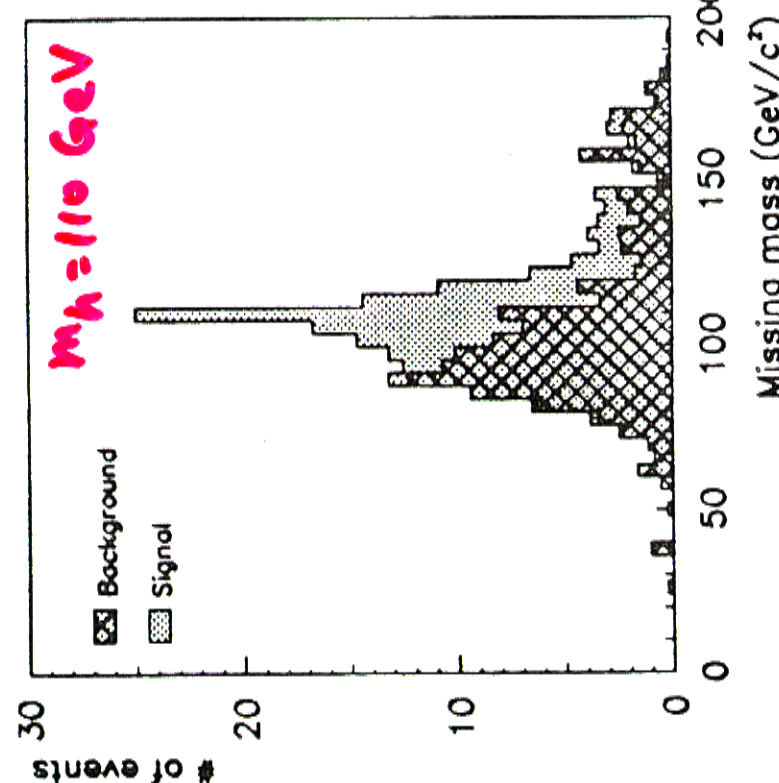


Figure 16: Distribution of the missing mass when the invisible decay is dominant for a Higgs boson mass of (a) $110 \text{ GeV}/c^2$ and (b) $140 \text{ GeV}/c^2$.

3.3 Can the standard model and the MSSM be disentangled?

and assuming a 100% $H^+ \rightarrow tb$ branching ratio. This extends the domain of the plane $(m_A, \tan \beta)$ where the charged Higgs bosons can be discovered up to $m_A \sim 200 \text{ GeV}/c^2$ (see Fig. 21), thus adding some redundancy for the distinction between the standard model and the MSSM, and for the possible identification of the MSSM.

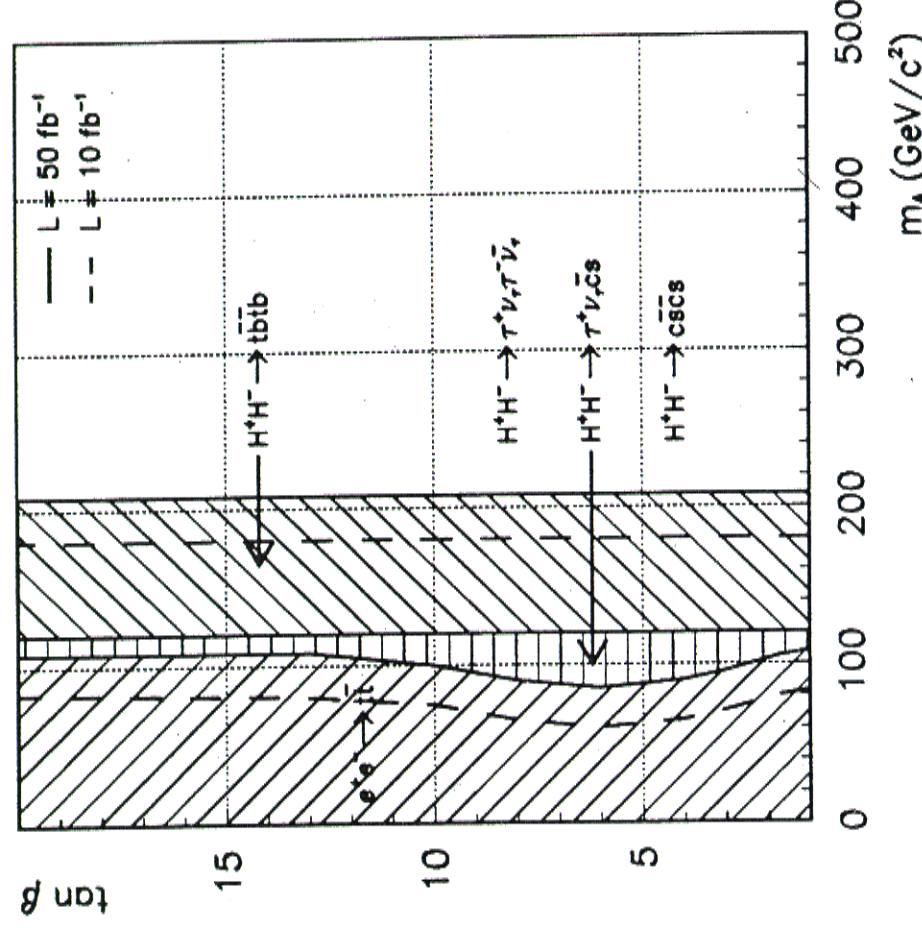


Figure 21: Domains of the $(m_A, \tan \beta)$ plane where the charged Higgs bosons of the MSSM can be discovered.

5 Conclusions

- discovery of h^0 guaranteed
- can also see H^0, A^0, H^+, H^-
if accessible

on more general grounds:

if Higgs not seen at LC
($\sqrt{s} = 500 \text{ GeV}, 50 \text{ fb}^{-1}$)
perturbative GUT excluded
w/ grand desert

caution

in the MSSM, heavy Higgs states
may well decay into SUSY particles

$$H^0, A^0 \rightarrow \tilde{\chi}^0 \tilde{\chi}^0, \tilde{\chi}^+ \tilde{\chi}^-, \tilde{t} \tilde{t}^*, \tilde{\tau}, \tilde{\tau}^*$$
$$H^\pm \rightarrow \tilde{\chi}^\pm \tilde{\chi}^0, \tilde{t} \tilde{b}^*$$

etc

all analyses change completely
in that situation

Study of Higgs properties

SM Higgs, $m_h > 2m_Z$

not much studied recently

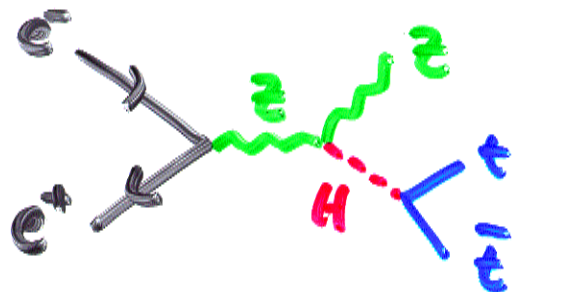
assumption

LHC finds $H \rightarrow ZZ \rightarrow l^+l^-l'^+l'^-$

possibly also $H \rightarrow W^+W^- \rightarrow l^+\nu_l l'^-\bar{\nu}_l$

You know what to look for

LC: $H \rightarrow t\bar{t}$, $Ht\bar{t}$ coupling



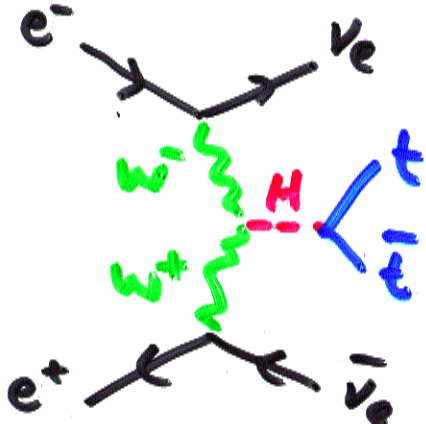
$\Rightarrow 8 \text{ jet!}$

Tanchi
et al

$m_H = 300 \text{ GeV}, m_t = 130 \text{ GeV}$

$\sqrt{s} = 600 \text{ GeV}, 60 \text{ fb}^{-1}$

$\Rightarrow \delta h_t/h_t = 10 \%$



$m_H = 600 \text{ GeV}, m_t = 150 \text{ GeV}$

$\sqrt{s} = 1 \text{ TeV}, 300 \text{ fb}^{-1}$

$\Rightarrow \delta h_t/h_t = 8 \%$

Tsukamoto

Fig.25 The cross sections for $e^+e^- \rightarrow t\bar{t}Z$ at $\sqrt{s} = 0.6$ (solid line) and 1.0 TeV(dashed line) for $m_t = 130$ GeV as functions of Higgs mass. For comparison, the cross sections for no Higgs case are also shown.

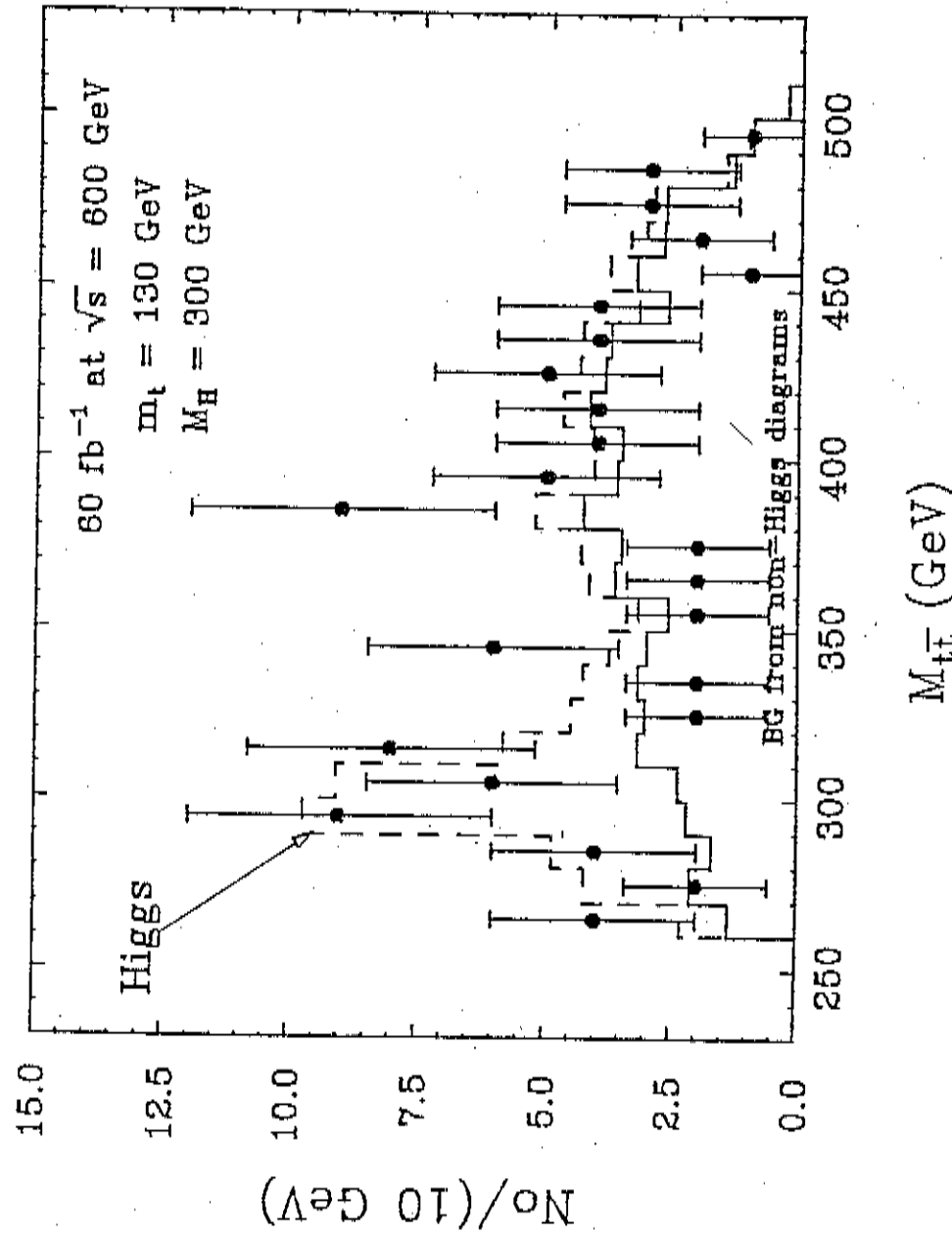


Fig.26 The invariant mass of the $t\bar{t}$ system for the process $e^+e^- \rightarrow t\bar{t}Z$, where $m_t = 130$ GeV, $M_H = 300$ GeV, and $\sqrt{s}=0.6$ TeV. Data points are Monte Carlo result corresponding to 60 fb^{-1} . The solid histogram is the background from non-Higgs diagrams, while the dashed includes the contribution from Higgs decays.

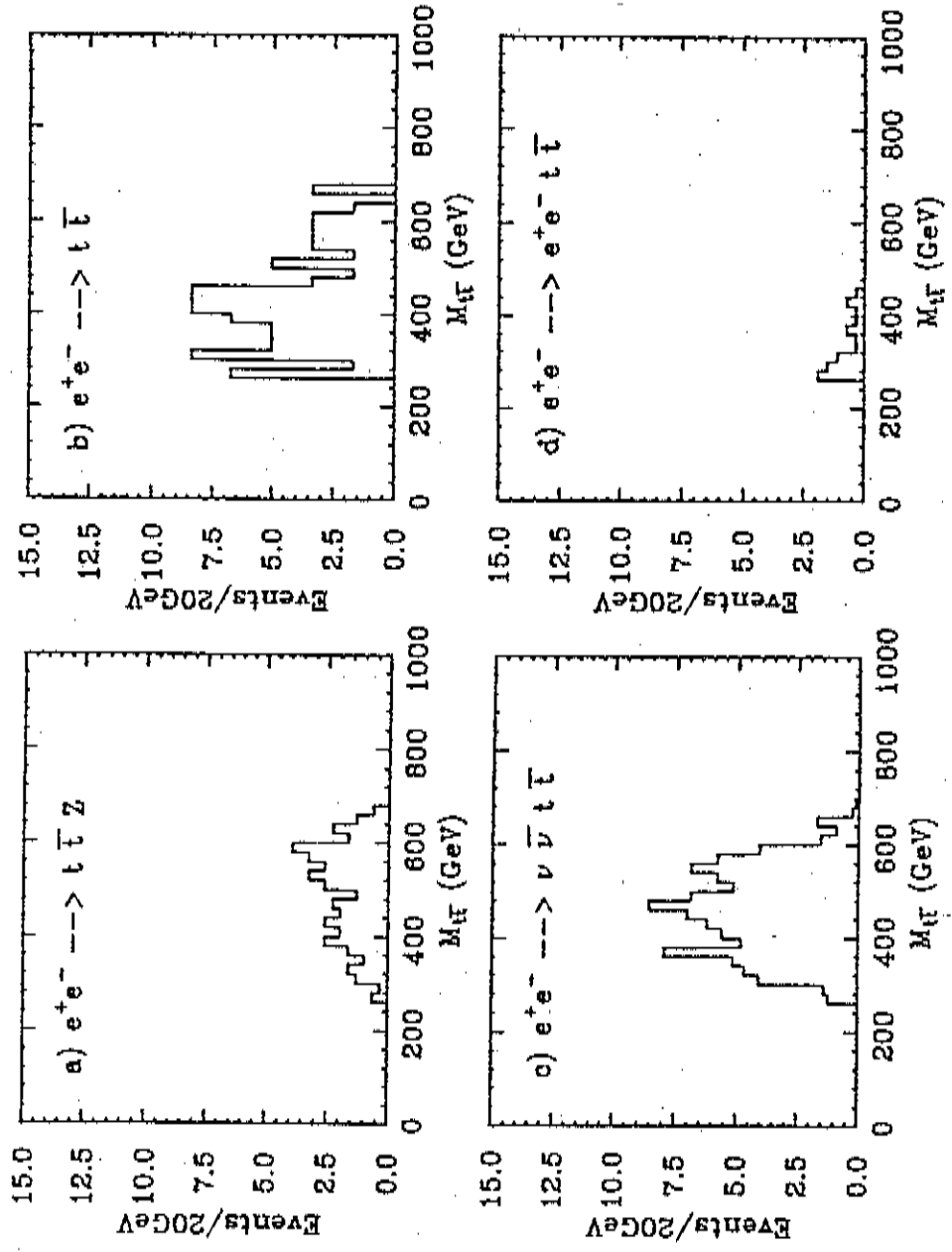


Fig.28 The invariant mass distributions for the $t\bar{t}$ system for (a) $e^+e^- \rightarrow t\bar{t}Z$, (b) $e^+e^- \rightarrow t\bar{t}$, (c) $e^+e^- \rightarrow \nu\bar{\nu}t\bar{t}$, and (d) $e^+e^- \rightarrow e^+e^- t\bar{t}$, where $m_t = 150$ GeV, $M_H = 600$ GeV, and $\sqrt{s} = 1.0$ TeV are assumed. The number of events corresponds to an integrated luminosity of 300 fb^{-1} .

test H is responsible for m_W, m_Z

$m_H = 500 \text{ GeV}$, $\sqrt{s} = 1 \text{ TeV}$, 60 fb^{-1}

\Rightarrow 70 signal, 80 BG events

$$\delta g_{WWH}/g_{WWH} \simeq 9\%$$

not optimized
higher \sqrt{s} helps

Study of Higgs properties

light SM or MSSM Higgs

Yamashita

$\mathcal{L} = 10 \text{ fb}^{-1}, 100 \text{ fb}^{-1}, 500 \text{ fb}^{-1}, 1000 \text{ fb}^{-1}$
 $\sqrt{s} = 300, 350, 400, 500 \text{ GeV}$

Bench Mark $M_H = 120 \text{ GeV}$

$\sqrt{s} = 300 \quad 350 \quad 400 \quad 500 \text{ GeV}$

$g_{ZZH}^2 \times$	ΔM_H	ΔBr	$\Delta \chi^2$
$\boxed{5}$	$6\% \quad < 3\% \quad - \quad 2.1\%$	$\mathcal{L} = 100 \text{ fb}^{-1}$ I. Nakamura et al	500 fb^{-1} W. Lohmann et al
$\boxed{\Delta M_H}$	$- \quad \pm 150 \text{ MeV} \quad - \quad \pm 300 \text{ MeV}$	$(ee, mu \text{ only})$ 500 fb^{-1} W. Lohmann	(4 jets) 10 fb^{-1} A. Just
$\boxed{\Delta Br}$	$2.5\% \quad 2.4\% \quad 7\% \quad 2.4\%$	bb I. Nakamura et al	500 fb^{-1} M. Battaglia et al
cc	$49\% \quad 13.5\% \quad - \quad 8.3\%$	"	M. Battaglia et al
gg	$23\% \quad 5.5\% \quad - \quad 5.5\%$	"	"
WW	$11.5\% \quad 5.1\% \quad 48\% \quad 5.1\%$	"	"
tt	$13.4\% \quad 5.7\% \quad 14\% \quad 5.7\%$	50 fb^{-1}	"
$cc + jj$	$15\% \quad - \quad 39\% \quad -$	"	
zz	$- \quad 14\% \quad 1000 \text{ fb}^{-1} \quad -$		D. Reid
Hvv $5 \times Br(Bb)$	$2.7\% \quad - \quad - \quad -$	100 fb^{-1} K. Ishii	

Recoil Mass Fit, $\mu^+ \mu^-$



García-Abia

Lohmann

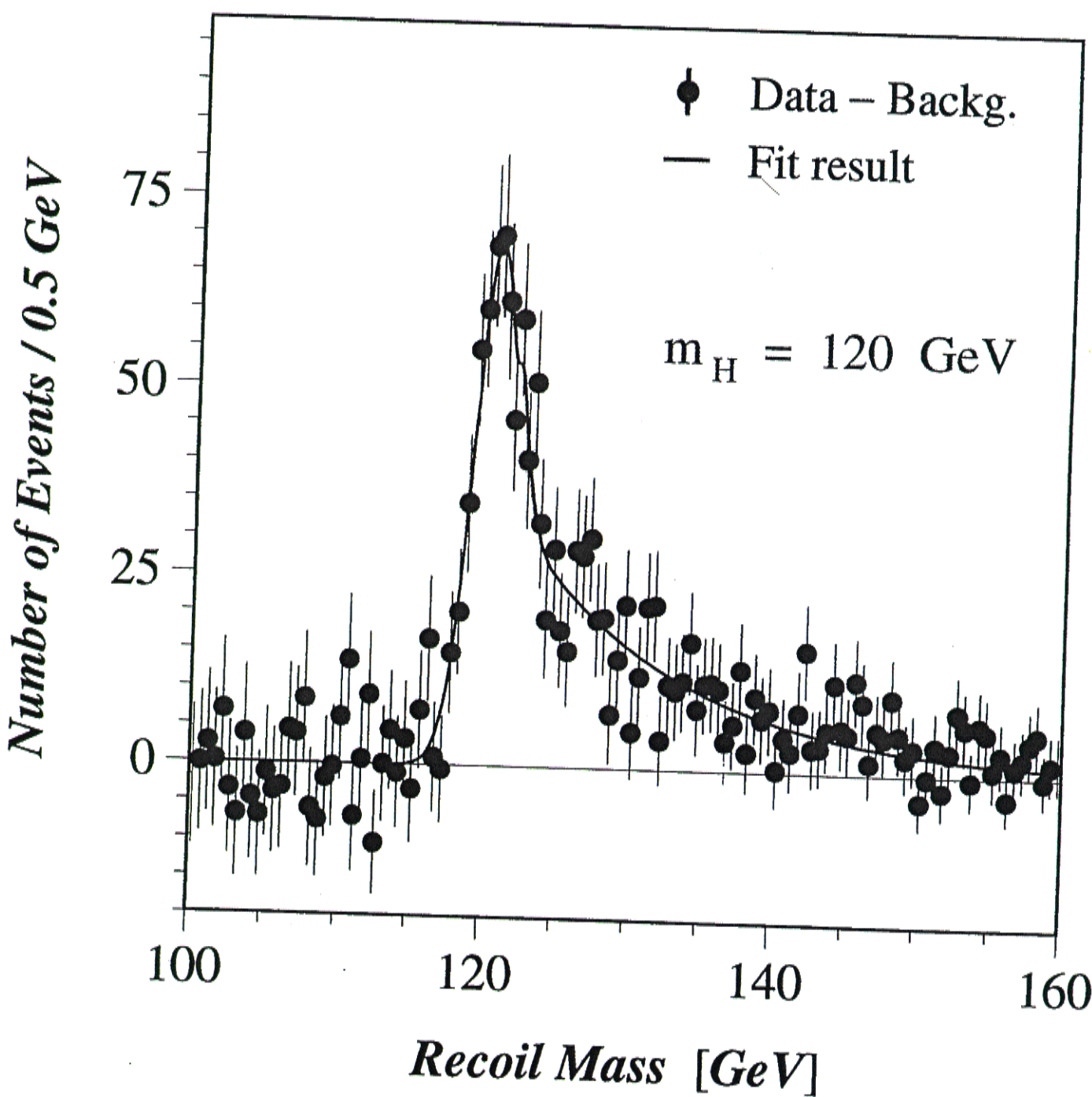
$\sqrt{s} = 350 \text{ GeV}$

$L = 500 \text{ fb}^{-1}$

$$M_H = 120.63 \pm 0.18 \text{ GeV}$$

$$\sigma_H = 1.62 \pm 0.15 \text{ GeV}$$

$$\sigma(ZH \rightarrow \mu^+ \mu^- X) = 5.35 \pm 0.21 \pm 0.13 \text{ fb}$$



Borisov, Richard

$H \rightarrow WW^* \rightarrow l\nu_2 g\bar{g}$

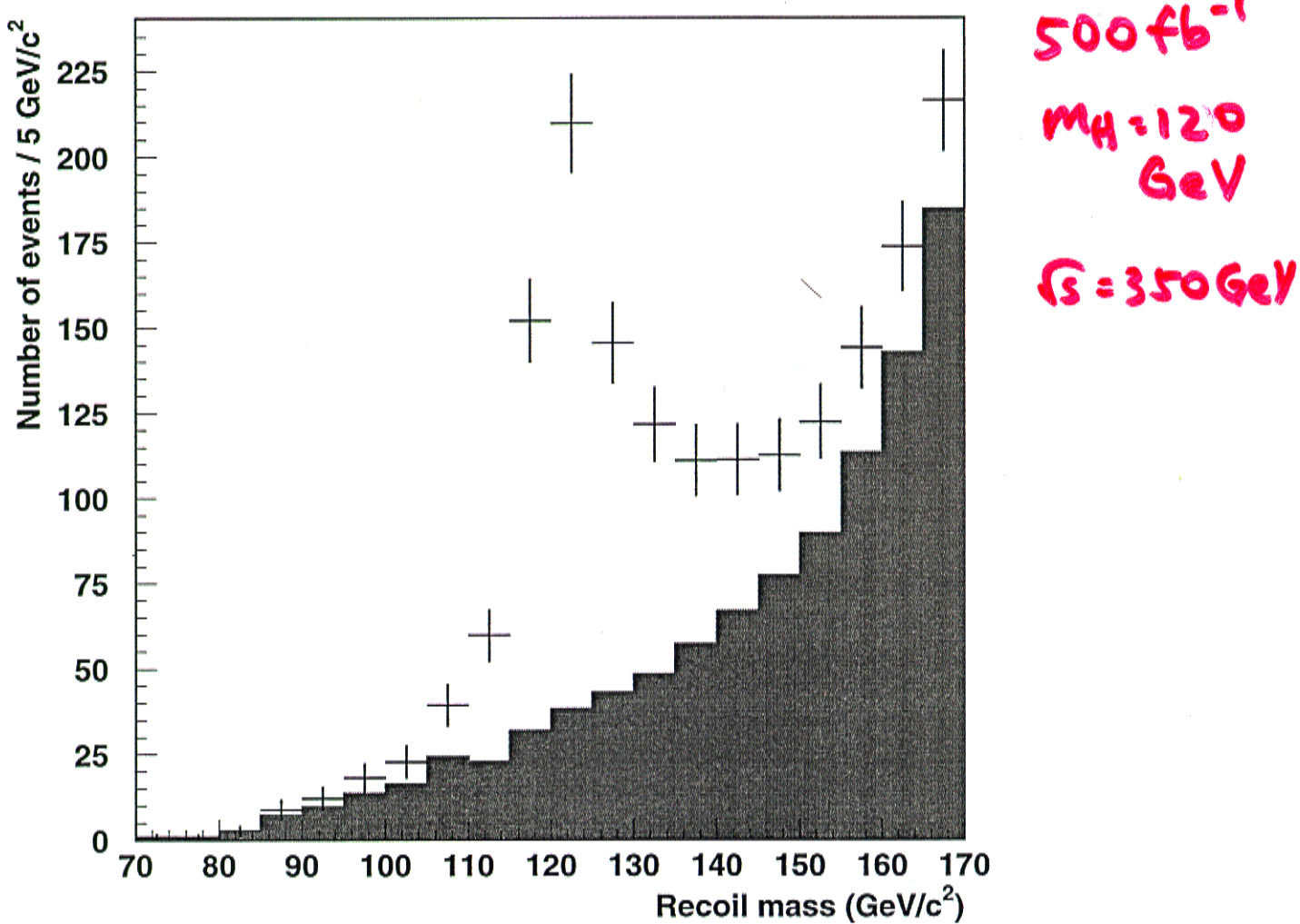
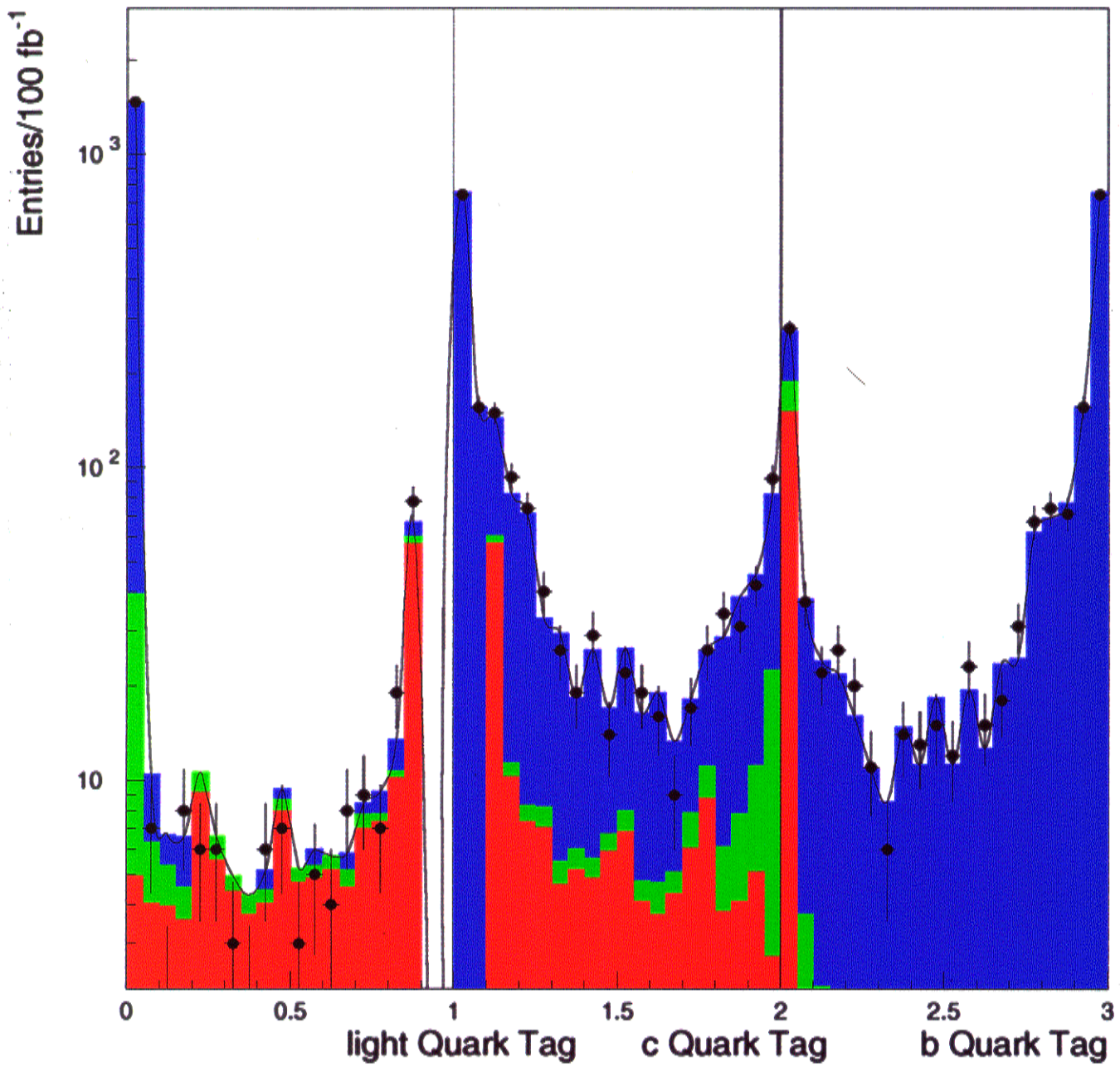


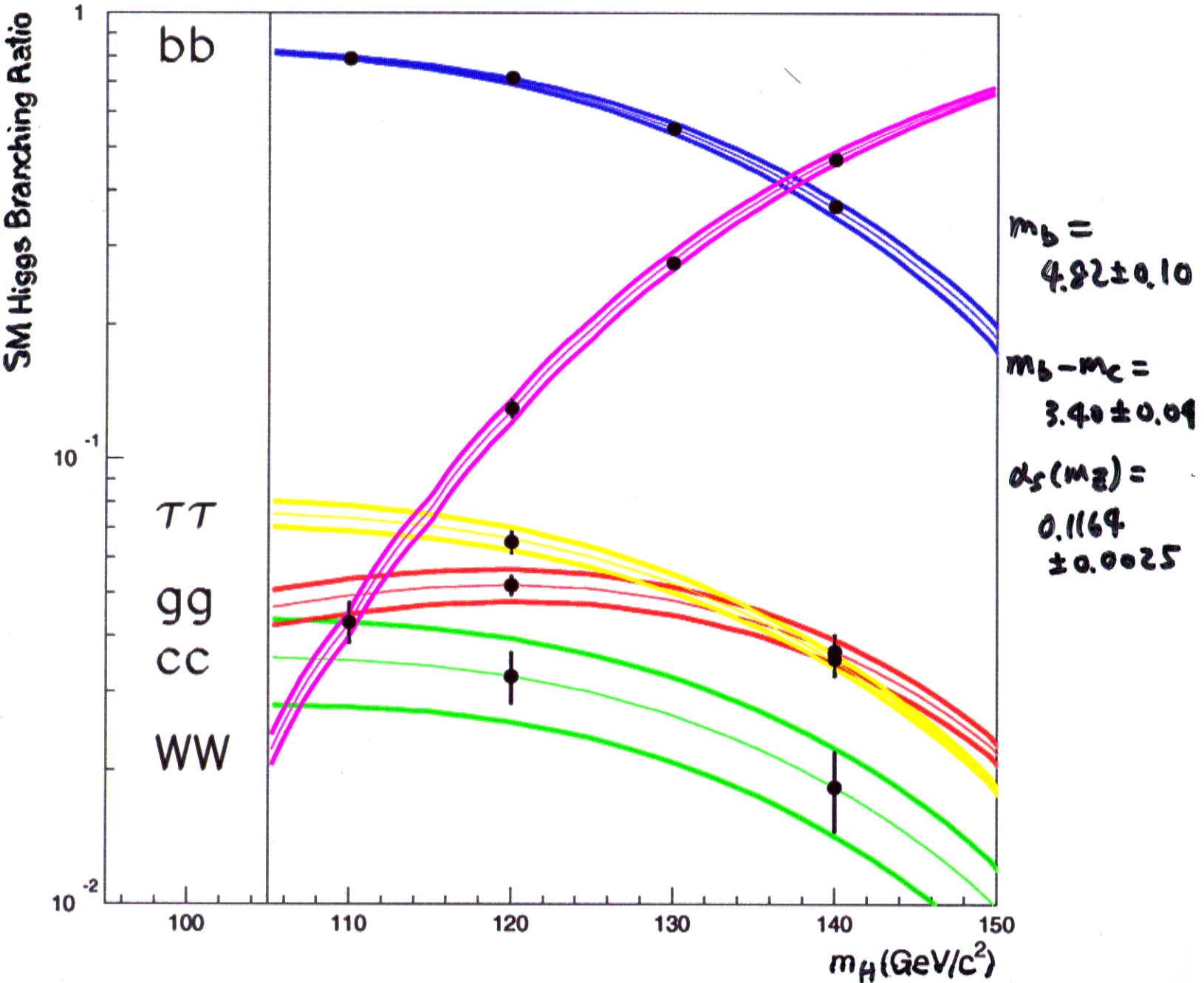
Figure 3: Expected distributions of the mass recoiling to any pair of jets with $|M_{jj} - M_Z| < 10$ GeV/c². The distribution is normalised to $\int L dt = 500$ fb⁻¹. The filled histogram shows the mass distribution for the background. The signal $h \rightarrow WW^*$ is generated with $M_H = 120$ GeV/c².



Higgs Branching Ratio Determination

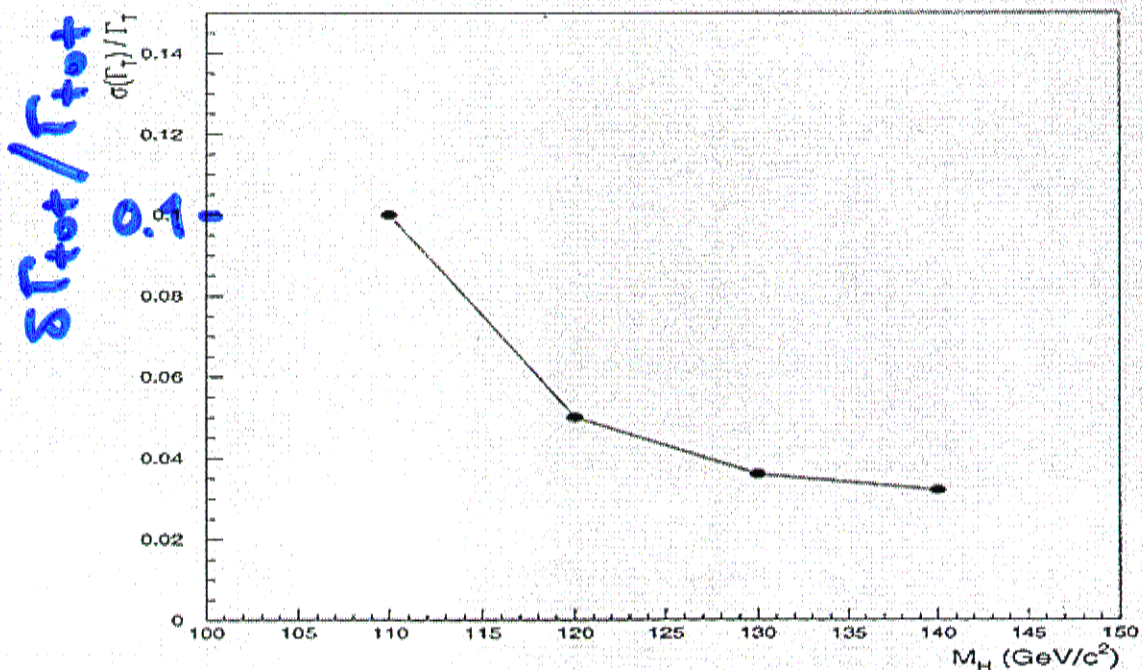
$m_H = 120 \text{ GeV}, 500 \text{ fb}^{-1}$

Channel	$\delta \left(\frac{\text{BR}(H \rightarrow X)}{\text{BR}(H \rightarrow \text{had})} \right) / \text{BR}$	$\delta \text{BR}(H \rightarrow X) / \text{BR}$		
$b\bar{b}$	1.1%	0.8%	2.4%	2.4%
$c\bar{c}$	13.4%	8.0%	13.5%	8.3%
gg	5.0%	5.0%	5.5%	5.5%
t^+t^-			6.0%	
WW^*			5.1%	
			350	500
			350	500



Deriving Γ_T^h

- Derivation of total Higgs decay width Γ_T^h usually relies on measuring $\text{BR}(H^0/h^0 \rightarrow \gamma\gamma)$ and $\sigma(\gamma\gamma \rightarrow h^0/H^0)$.
- Precise determination of $\text{BR}(H^0/h^0 \rightarrow WW^*)$ may provide alternative means for deriving Γ_T^h :
 - $\text{BR}(h \rightarrow WW^*) = \frac{\Gamma_{WW^*}}{\Gamma_{tot}}$
 - Measure $\text{BR}(h \rightarrow WW^*)$
 1. from σ_{ZH} estimate $\Gamma_{WW^*} \simeq \Gamma_{ZZ^*}$ assuming coupling universality
 2. from WW fusion $e^+e^- \rightarrow \nu\bar{\nu}WW^* \rightarrow \nu\bar{\nu}h^0$ extract Γ_{WW^*}
 3. from $\Gamma_{WW^*}^{SM}$ estimate $\Gamma_{WW^*} \simeq \Gamma_{WW^*}^{SM}$.

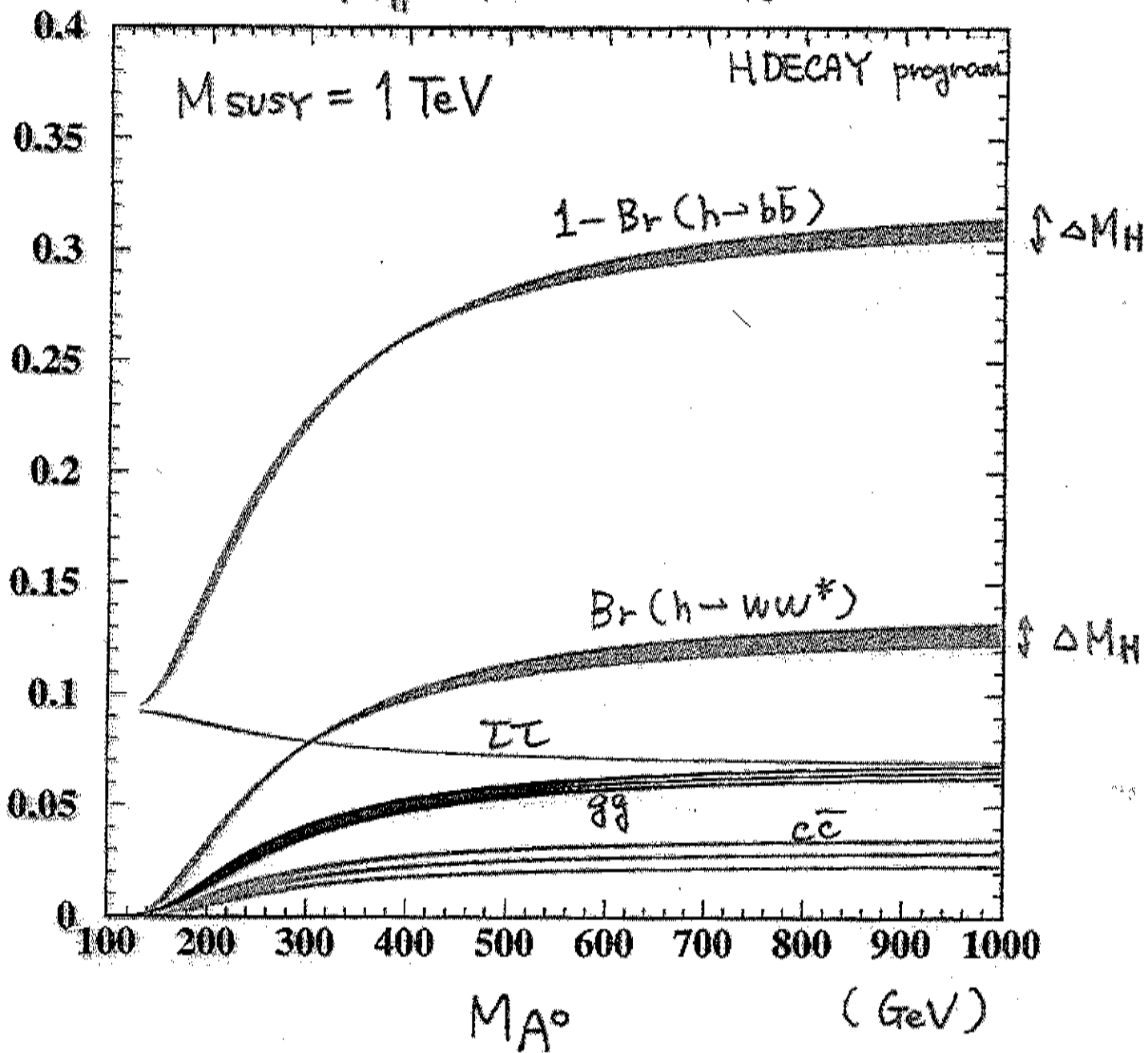


MH

Kamoshita, Okada, Tanaka

Yamashita

$$M_{h^0} = 120 \pm 0.5 \text{ GeV}$$



SCAN OF MSSM PARAMETER SPACE

- Scan of MSSM parameters:

$$\begin{aligned}
 2 < \tan \beta < 60 \\
 150 \text{ GeV}/c^2 < M_A < 1100 \text{ GeV}/c^2 \\
 500 \text{ GeV}/c^2 < M_{SUSY} < 1500 \text{ GeV}/c^2 \\
 -1000 \text{ GeV} < \mu < 1000 \text{ GeV} \\
 0 < M_{LR}^t/M_{\tilde{q}} < \sqrt{6} \\
 0.5 < M_{\tilde{g}}/M_{SUSY} < 1
 \end{aligned}$$

- find MSSM parameters giving $M_{h^0} = (120 \pm 2) \text{ GeV}/c^2$ using the diagrammatic two-loop result for M_h by Heinemeyer, Hollik, Weiglen implemented in the FEYNHIGGS program,
- compute Higgs decay branching ratios, including QCD corrections for quark and squark loops computed by Djouadi, Kalinowski, Spira and implemented in the HDECAY program.
- compute pulls of MSSM BR's from those predicted in SM:

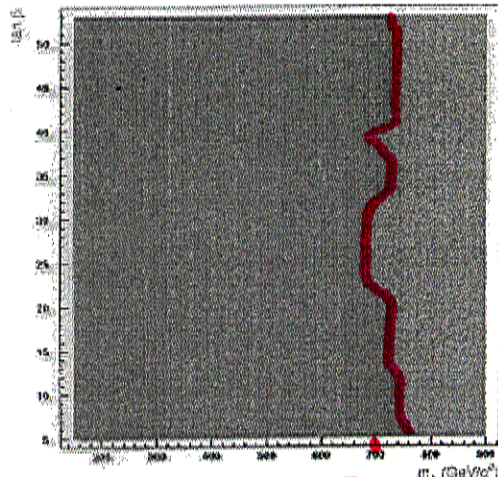
$$\Delta(BR) = \frac{|BR^{\text{MSSM}} - BR^{\text{SM}}|}{\sqrt{\sigma_{th}^2 + \sigma_{exp}^2}}$$

- choose as discriminating variables:

1. $\text{BR}(h \rightarrow b\bar{b})/\text{BR}(h \rightarrow \text{hadrons})$
2. $\text{BR}(h \rightarrow c\bar{c})/\text{BR}(h \rightarrow \text{hadrons})$
3. $\text{BR}(h \rightarrow g\bar{g})/\text{BR}(h \rightarrow \text{hadrons})$
4. $\text{BR}(h \rightarrow b\bar{b})/\text{BR}(h \rightarrow WW^*)$

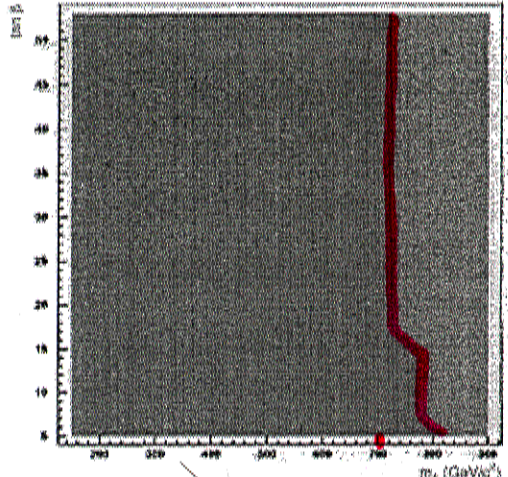
SM / MSSM SEPARATION IN M_A - $\tan\beta$ PLANE
 $\int L = 1000 \text{ fb}^{-1}$, THEORY SYST. / 2.0

CDR VERTEX TRACKER
 TESLA $L = 1000 \text{ fb}^{-1}$



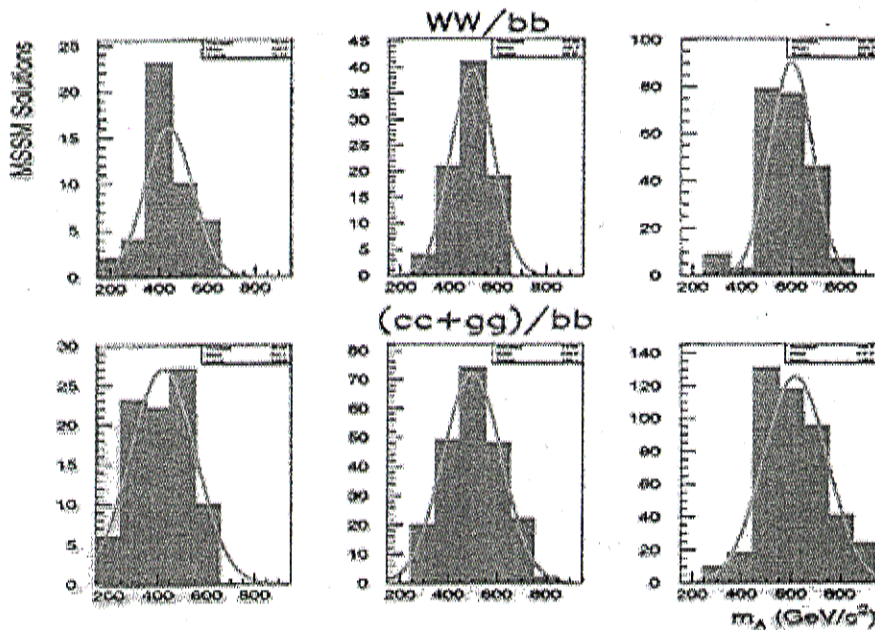
700 M_A

IMPROVED VERTEX TRACKER
 TESLA $L = 1000 \text{ fb}^{-1}$



700 M_A

SENSITIVITY TO M_A



Higgs Studies at the e^+e^- Linear Collider-

luminosity crucial?

not necessarily ...

if purely statistics limited:

$$\frac{BR(h \rightarrow c\bar{c})}{BR(h \rightarrow b\bar{b})} \cong \frac{BR(h \rightarrow c\bar{c})|_{SM}}{BR(h \rightarrow b\bar{b})|_{SM}} \times \left(1 - 2 \underbrace{\frac{m_h^2 + m_A^2}{m_A^2}}_{\sim 1/\sqrt{N}}\right)$$

limit on $m_A \sim N^{1/4}$

if purely systematics limited:

limit on $m_A \sim N^0$

Needs to be redone w/ smaller lumi'

degradation in sensitivity

probably not very dramatic

Yamashita

$M_H = 120 \text{ GeV}$ $\mathcal{L} = 200 \text{ fb}^{-1}$ LCWS'99
compilation

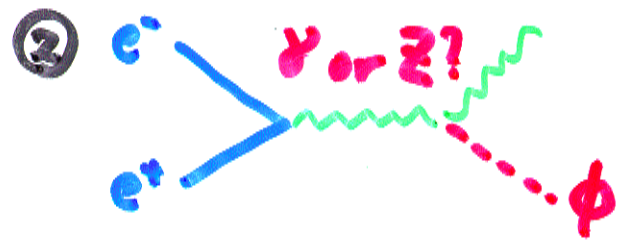
	$\sqrt{s} = 300 \text{ GeV}$	350 GeV	500 GeV	
$\frac{\Delta Q}{Q}$	4.2%	4.7%	3.3%	$\Rightarrow 4\%$
ΔM_W	—	230 MeV (ee, $\mu\mu$ only)	60 MeV (4 jet)	$\Rightarrow 60 \text{ MeV}$
$\frac{\Delta p_T}{p_T}$				
W	1.8%	3.8%	3.8%	$\Rightarrow 2\%$
W'	8%	8%	8%	$\Rightarrow 8\%$
T	7%	9%	9%	$\Rightarrow 7\%$
W_{miss}	10%	—	—	$\Rightarrow 10\%$
e	35% (I.P. only)	21%	13%	$\Rightarrow 15\%$
$\tau\tau$	16% (I.P. only)	8%	8%	$\Rightarrow 8\%$
$\pi\pi$	—	14%	—	
		$(\mathcal{L} = 1000 \text{ fb}^{-1})$		

Similar numbers
~ independent to \sqrt{s} ?

$m_h \sim 130$ GeV, $\sqrt{s} \sim 300$ GeV, 50fb^{-1}

$\sigma \sim 200$ fb 10K events

completely model-indep study
to determine the nature
of the discovered particle.



pol asymm

$$-0.14 \pm 0.06$$

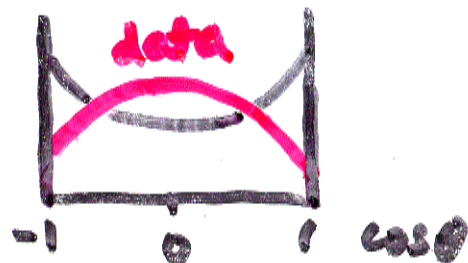
Z

③ scalar or pseudo-scalar?

$$\phi_s Z^\mu Z^\nu$$

$$\phi_{PS} Z^\mu \tilde{Z}^\nu$$

scalar



2.3.2 Spin and parity determination

50 fb⁻¹, $\sqrt{s} = 500 \text{ GeV}$

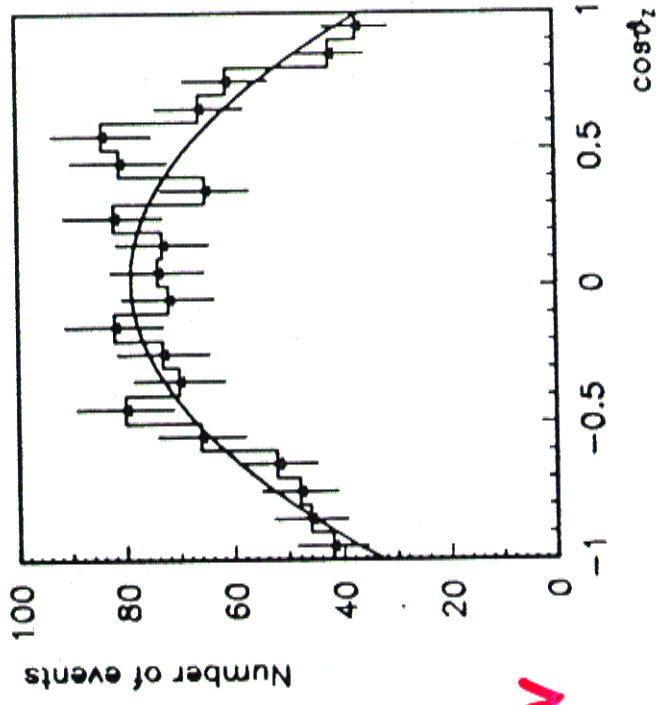


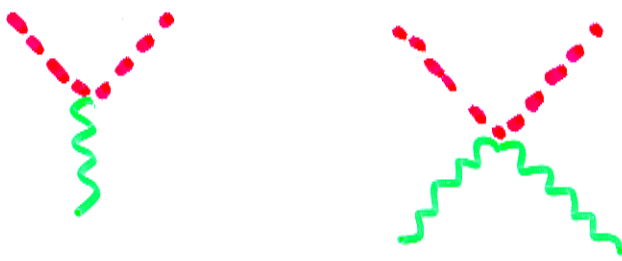
Figure 8:
Angular distribution of the Z with 50 fb^{-1} .

2.3.3 Cross-section measurement

The cross-section of the process $e^+e^- \rightarrow HZ$, and therefore the HZZ coupling can be measured by counting the number of events selected in the leptonic channel, since the selection criteria and the mass reconstruction are independent of the Higgs boson decay mode. With 50 fb^{-1} , the 150 signal events expected over an almost negligible background

If $m_H^2, m_Z^2 \ll \sqrt{s}$, which is approximately the case at 500 GeV, the angular distribution of the Zs produced in $e^+e^- \rightarrow HZ$ is proportional to $\sin^2 \theta$. This distribution is shown in Fig. 8 in the four-jet topology after background subtraction, for $m_H = 110 \text{ GeV}/c^2$, with 50 fb^{-1} actually taken at 300 GeV. Furthermore, since these Zs are essentially longitudinally polarized, the angular distribution of the decay products in the Z rest frame is also proportional to $\sin^2 \theta$ [15]. These measurements unambiguously characterizes a $J^P = 0^+$ particle and can be done with much less than 50 fb^{-1} .

$\phi Z_\mu Z^\mu$ coupling



$$\langle \phi \rangle$$

$$\rightarrow \langle \phi \rangle \neq 0$$

$$\langle \phi \rangle_x$$

→ contributes to m_Z

all of it?

part of it?

→ 3% measurement of $\dots \rightarrow Z$ Janet

if only a part: more Higgs bosons

what about m_W ?

→ $e^+ e^- \rightarrow h$

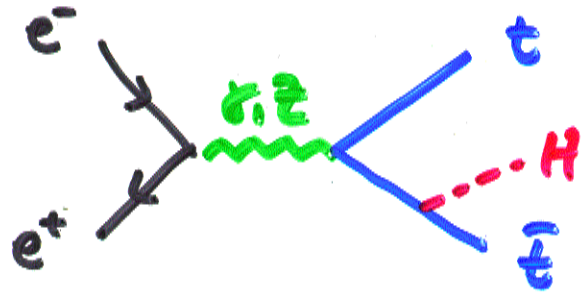
$\dots h \sim 4-10\%$ measurement

Janet

$50fb^{-1}$

$\sqrt{s} = 500 GeV$

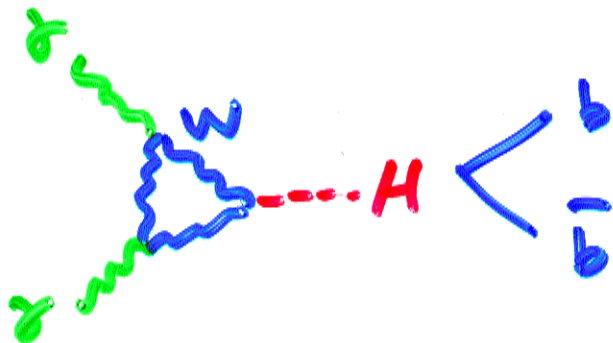
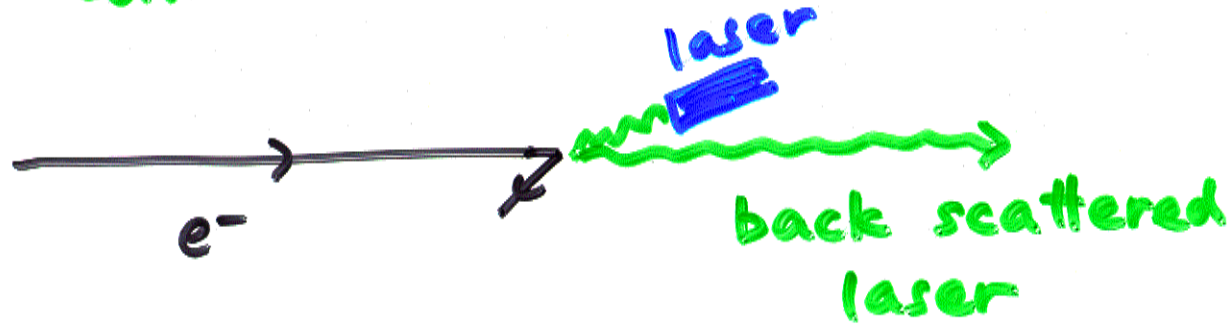
$t\bar{t}H$ coupling



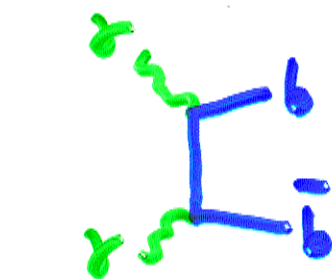
$$\left. \begin{array}{l} \sqrt{s} = 500 \text{ GeV} \\ m_H < 110 \text{ GeV} \\ 50 \text{ fb}^{-1} \end{array} \right\} \Rightarrow \frac{\delta g_{t\bar{t}H}}{g_{t\bar{t}H}} \lesssim 10\%$$

Reina

$\gamma\gamma$ collider

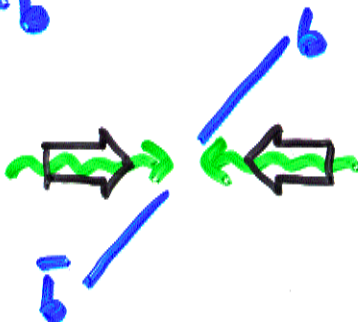


BG:



trick

$$J_Z = 0$$



$$\propto m_b^2/s$$

helicity suppression

$b\bar{b}g$ still serious BG

$$\sigma(\gamma\gamma \rightarrow H \rightarrow b\bar{b}) \propto \Gamma(H \rightarrow tt) \cdot BR(H \rightarrow b\bar{b})$$

15 fb^{-1}

$\Delta m_{b\bar{b}} = 10 \text{ GeV}$

Melles

5

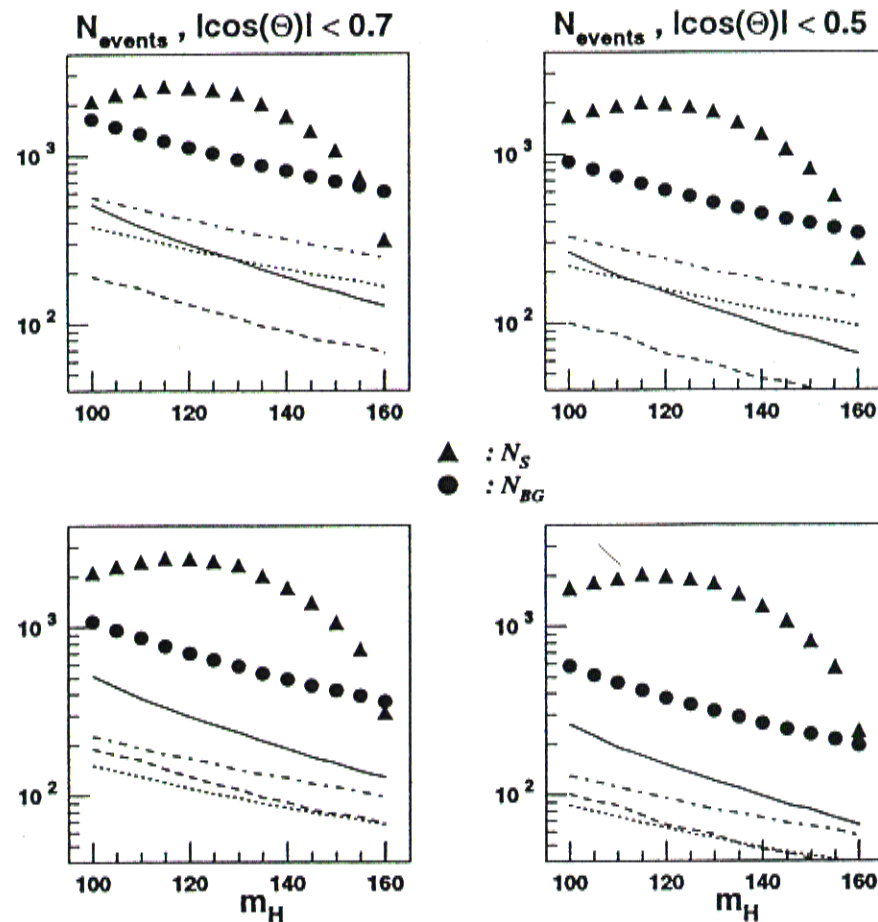


Figure 4. The number of both signal and background events for jet parameters $\epsilon = 0.1$ and $\delta = 20^\circ$ and the indicated values of the thrust angle θ . The upper row assumes a ratio of $J_0/J_2 = 20$ and the lower row of 50. The background is composed of bottom and charm contributions assuming 70 % double b-tagging efficiency and a 3 % probability to count a $c\bar{c}$ pair as $b\bar{b}$. The dash-dot line corresponds to $J_z = \pm 2$ for m_c , the full line to $J_z = 0$ for m_b , the dotted line to $J_z = \pm 2$ for m_b and the dashed line to $J_z = 0$ for m_c . All lines are normalized to add up to the total background and all radiative corrections discussed in the text are included.

differing cuts on the jet thrust angle θ . One can

the Sterman-
this work. In
try hard gluon
lation outside
gluon energy is
incident center
denoted by θ .

important check
phase space and
of Ref. [10].

branching ra-
here we use the
[3], and include
 W^* , ZZ^* and
radiative cor-

rst (conserva-
lly achievable
the Tesla de-

Melles

different cuts

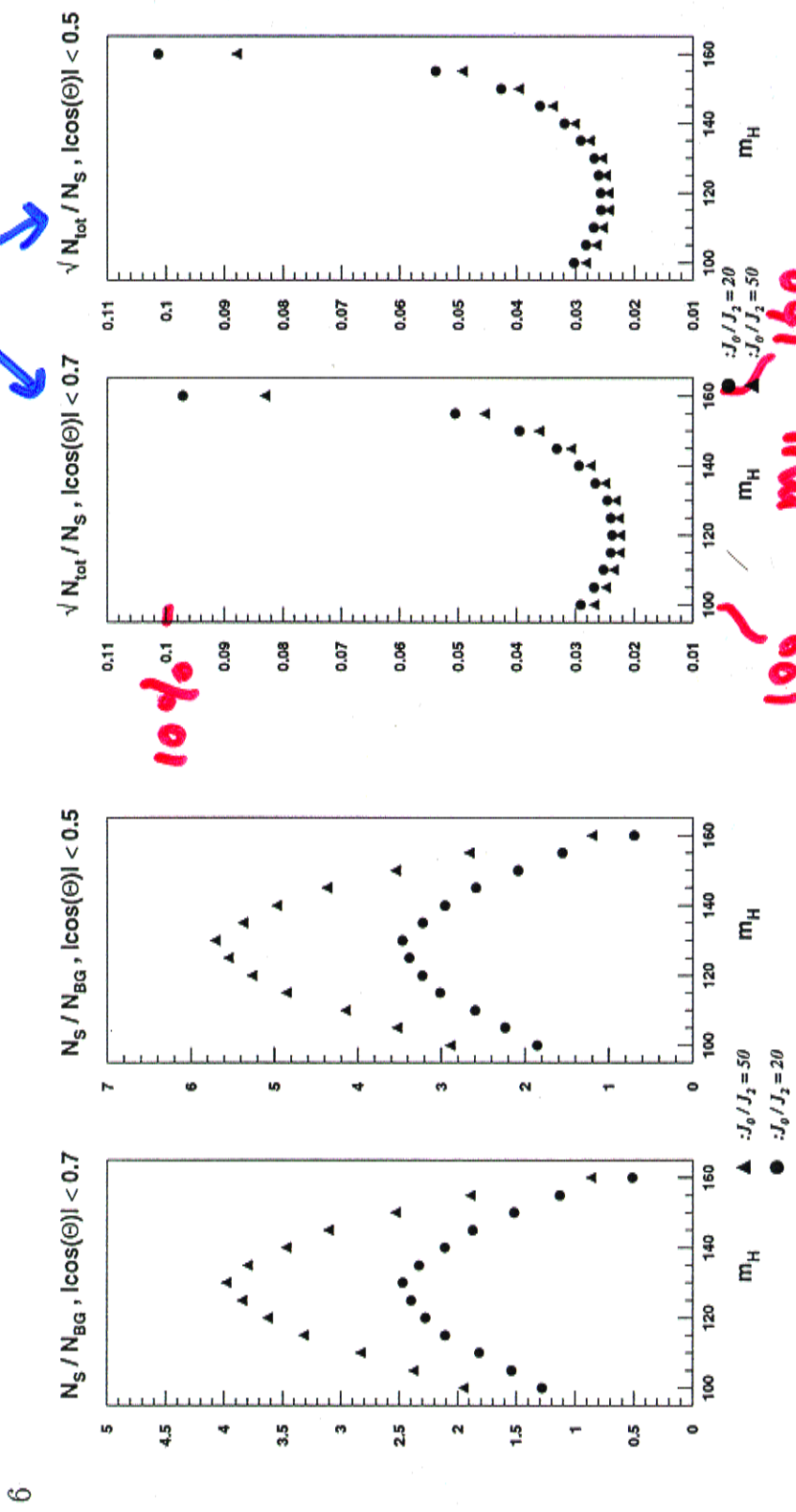


Figure 5. The ratio of signal to background events based on the jet parameters of Fig. 4. The smaller phase space cut $|\cos \theta| < 0.5$ gives a larger ratio as expected.

4. Conclusions

In this paper we have included all available and relevant radiative corrections for the measurement of the partial Higgs width $\Gamma(H \rightarrow \gamma\gamma)$. Conservative assumptions about the ex-

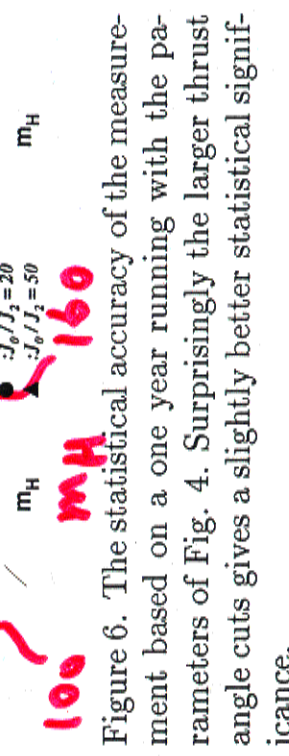


Figure 6. The statistical accuracy of the measurement based on a one year running with the parameters of Fig. 4. Surprisingly the larger thrust angle cuts gives a slightly better statistical significance.

REFERENCES

1. I.F. Ginzburg et. al., Nucl.Inst.Meth. **205** (1983) 47 & Nucl.Inst.Meth. **219** (1984) 5.
2. V.I. Telnov, Nucl.Inst.Meth. **A 355** (1995) 5.
3. M. Spira, hep-ph/9705337, Fortsch.Phys. **46** (1999) 100.

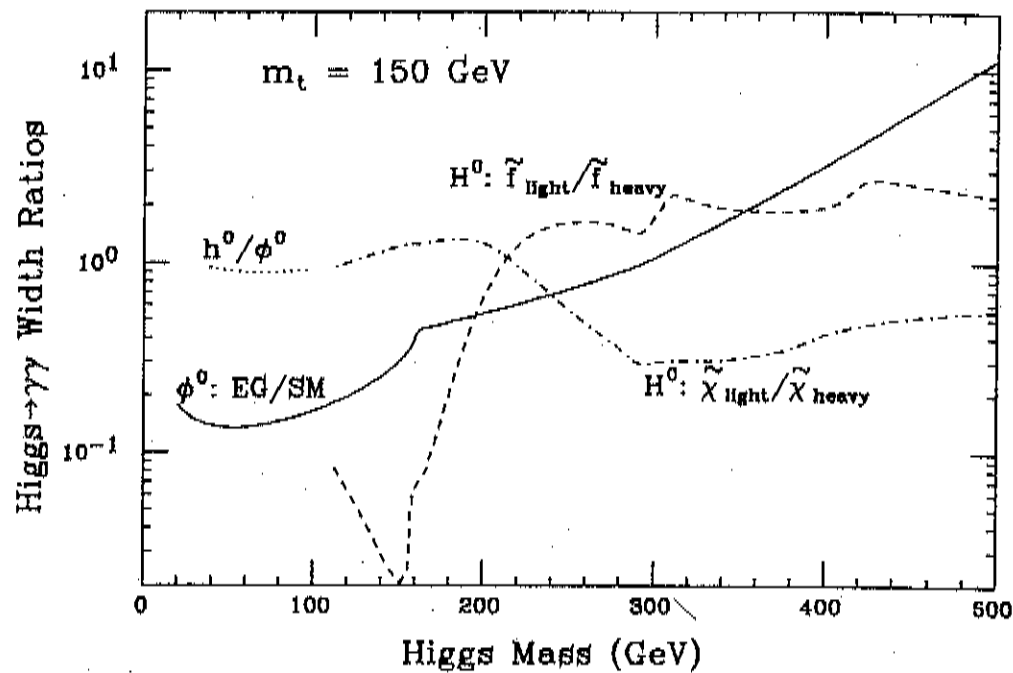


Figure 1: The ratio of $\Gamma(\text{Higgs} \rightarrow \gamma\gamma)$ computed for two different model choices for a number of cases. In the case of the ϕ^0 , the ratio of the width predicted in the presence of an extra heavy generation to that obtained in the MSM is shown. For the h^0 , the ratio $\Gamma(h^0 \rightarrow \gamma\gamma)/\Gamma(\phi^0 \rightarrow \gamma\gamma)$ as a function of $m_{h^0} = m_{\phi^0}$ with $m_{A^0} = 400$ GeV is plotted. Squarks and charginos have been taken to be as light as possible without being observable at the $\sqrt{s} = 500$ GeV collider. For the H^0 two curves are shown. The dot-dashed curve is $\Gamma(H^0 \rightarrow \gamma\gamma)$ in a model with light charginos ($M = -\mu = 150$ GeV in the notation of Ref. 2) divided by the corresponding width with heavy charginos ($M = -\mu = 1$ TeV), keeping the squarks and sleptons heavy (with masses of order 1 TeV). The dashed curve is $\Gamma(H^0 \rightarrow \gamma\gamma)$ in a model with light squarks and sleptons (given by a common soft-SUSY breaking diagonal mass of 150 GeV for all squarks and sleptons, with all off-diagonal mass terms set to zero) divided by the corresponding width computed with heavy squarks and sleptons, keeping the charginos heavy (as specified above). For the latter two curves, the ratio of widths is plotted as a function of m_{H^0} for $\tan\beta = 2$. The top quark mass is taken equal to 150 GeV for all calculations. This figure is taken from Ref. 12.

1-loop contribution of a charged particle with mass $\gtrsim m_{\phi^0}/2$, approaches a constant value that depends upon whether it is spin-0, spin-1/2, or spin-1. (The contributions are in the ratio $-1/3 : -4/3 : 7$, respectively.) For a light Higgs boson, in the MSM the dominant contribution is the W -loop diagram. The next most important contribution is that from the top quark loop, which tends to cancel part of the W -

$\tan\beta$ measurement ($m_A \gg m_Z$)

$$H^0 \rightarrow b\bar{b} \propto \frac{\cos\alpha}{\cos\beta} \rightarrow \tan\beta$$

$$H^0 \rightarrow t\bar{t} \propto \frac{\sin\alpha}{\sin\beta} \rightarrow \frac{1}{\tan\beta}$$

$$A^0 \rightarrow b\bar{b} \propto \tan\beta$$

$$A^0 \rightarrow t\bar{t} \propto \frac{1}{\tan\beta}$$

$$H^+ \rightarrow t\bar{b} \propto \frac{m_t}{\tan\beta} (1 + \delta_5) + m_b \tan\beta (1 - \delta_5)$$

$$\frac{BR(H^+ \rightarrow \tau^+\nu_\tau)}{BR(H^+ \rightarrow t\bar{b})} \text{ good for } \tan\beta = 3 - 10$$

$$\sigma(e^+e^- \rightarrow t\bar{b} H) \text{ good for } \tan\beta \gtrsim 40$$

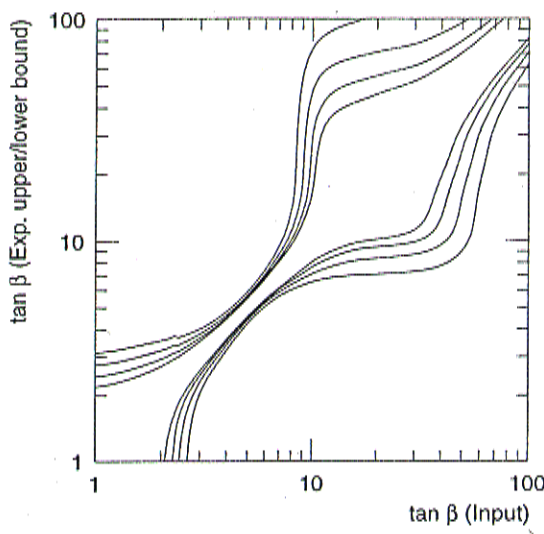


Figure 1: Accuracy of the measured $\tan \beta$ (95 % C.L.) for $\sqrt{s} = 500$ GeV, $m_{H^\pm} = 200$ GeV, $\epsilon_b = 60$ %, and four integrated luminosities: 25, 50, 100, and 200 fb^{-1} (from outside to inside).

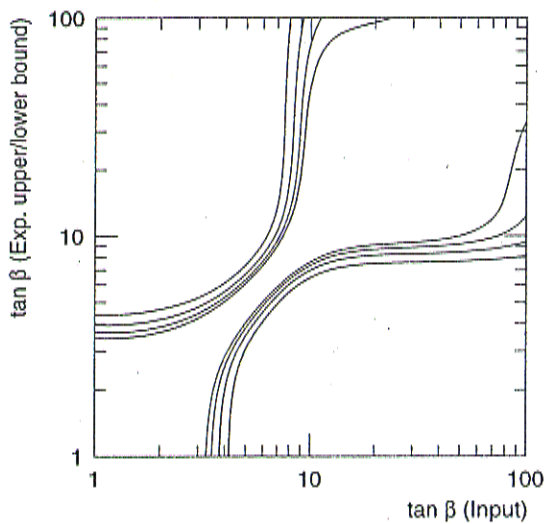
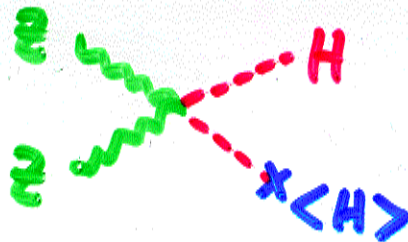


Figure 4: Same as Fig. 2, except for $m_{H^\pm} = 400$ GeV.

Evidence for Higgs condensate



⇒ proves the origin of m_W, M_Z

$H \rightarrow f\bar{f}$ branching fractions

$$BR(H \rightarrow f\bar{f}) \propto m_f^2$$

$b\bar{b}/\tau^+\tau^-$ ratio the same
in the MSSM

$c\bar{c}$ tests the deviation
from the SM

$H \rightarrow \gamma\gamma, gg$ constrains new physics

e.g. 4th gen $\Rightarrow \Gamma(H \rightarrow gg) \times 9$

SUSY loop

$\tan\beta, h_{tth}$ measurements

Draw Your Own Conclusion